The influence of heavy metal stress on the evolutionary transition of teosinte to maize

Jonathan Acosta-Bayona[1], Miguel Vallebueno-Estrada[2], and Jean-Philippe Vielle-Calzada[1]*

[1]Grupo de Desarrollo Reproductivo y Apomixis, Unidad de Genómica Avanzada Langebio, Centro de Investigación y de Estudios Avanzados del IPN, Km 9.6 Libramiento Norte Carretera Irapuato-León, CP36825 Irapuato Guanajuato, México

[2]Swedish University of Agricultural Sciences, Umeå, Sweden

*Author for correspondence:
Jean-Philippe Vielle-Calzada
Tel: 421663000 ext. 3100
Email: vielle@cinvestav.mx

ORCIDs
Acosta-Bayona: https://orcid.org/0009-0005-7305-6245
Vallebueno-Estrada: https://orcid.org/0000-0001-8647-8758
Vielle-Calzada: https://orcid.org/0000-0002-3017-2490

Summary

Maize originated from teosinte *parviglumis* following a subspeciation event occurred in volcanic regions of Mesoamerica. The elucidation of the phenotypic changes that gave rise to maize have focused on the direct consequences of domestication, with no insights on how environmental factors could have influenced specific gene function and human selection. The genome of the *Palomero toluqueño* landrace suggested heavy metal (HM) effects on maize domestication (Vielle-Calzada et al., 2009). To test the hypothesis that HM stress influenced the evolutionary transition of teosinte to maize, we exposed both subspecies to sublethal concentrations of copper and cadmium. We also assessed the genetic diversity of three HM response genes mapping to chromosome 5 (chr.5) and previously shown to be affected by domestication: *ZmHMA1*, *ZmHMA7* – encoding for heavy metal ATPases of the $P1_b$ family-, and *ZmSKUs5,* encoding for a multicopper oxidase. *ZmHMA1* and *ZmSKUs5* are within a genomic region containing hundreds of genes linked to QTLs with pleiotropic effects on domestication. The genomic analysis of chr.5 shows that the three genes were under strong positive selection as compared to previously identified domestication genes. Large-scale transcriptomic comparisons indicate that many other loci containing HM response genes were also positively selected across the maize genome. Exposure of teosinte *parviglumis* to HM stress results in a plant architecture reminiscent of extant maize, and upregulation of *Teosinte branched1* (*Tb1*) in the meristem. *ZmHMA1* and *ZmHMA7* are expressed throughout development and respond to HM stress in both subspecies. *ZmHMA1* is mainly involved in restricting plant height and optimizing the number of female inflorescences and seminal roots. Paleoenvironmental studies reveal a temporal and geographical convergence between volcanic eruptions and maize emergence during the early Holocene, at periods of climatic instability. Overall, these results suggest that abiotic stress influenced the evolutionary transition that gave rise to extant maize through the activity of heavy metal response genes and their phenotypic effects, as a possible consequence of volcanic activity.

Key words: maize, teosinte *parviglumis*, heavy metals, domestication, ATPases, seminal roots.

Introduction.

Driven by either conscious or unconscious human selection, domestication can be considered a gradual evolutionary process resulting in the adaptation to agroecological environments and anthropogenic preferences (Ross-Ibarra et al. 2007). In the case of plants, the obvious consequences of domestication are represented by visually recognizable traits that include changes in photoperiod response, reduced capacity of seed dispersion, reduced lateral branching, larger fruits or grains, reduced duration of seed dormancy, and increase in the size of female inflorescences (Pickersgill 2007; Larson et al. 2014). Notably, research efforts to understand the phenotypic changes that gave rise to maize have mainly focused on the direct consequences of domestication in aerial organs and sometimes roots (Chen et al. 2022; Lopez-Valdivia et al. 2022; Ren et al. 2022), with no emphasis on the role of adaptive environmental responses that, by acting on specific gene function, could have given rise to phenotypic traits that were identified and selected by humans.

It is generally accepted that domestication of maize (*Zea mays* ssp. *mays*) from teosinte *parviglumis* (*Zea mays* ssp. *parviglumis*) initiated in Mesoamerica around 9,000 years before present (Matsuoka et al. 2002). The initial evolutionary transition that resulted in the event of subspeciation most likely occurred close to the Balsas river drainage, in regions geographically converging with the Trans-Mexican Volcanic Belt (TMVB), at the intersection of the States of Mexico, Guerrero, and Michoacan (Matsuoka et al. 2002). Although the nature of the initial phenotypic changes that allowed the emergence of primitive maize remains unclear, the most obvious architectural and morphological differences between both subspecies affect their vegetative and reproductive organs. Teosinte *parviglumis* generates numerous lateral branches ending in male inflorescences, while maize often has a few short or no lateral branches, not ending in male reproductive organs (Wills et al. 2013). Additionally, the seeds of teosinte *parviglumis* are covered by a hard glume that protects the kernel externally, while in maize glumes are reduced, soft and do not cover the kernel (Doebley and Stec 1993). Large scale efforts involving physical mapping and comparative genomic analysis have resulted in the identification of numerous regions showing differential nucleotide variability between teosinte *parviglumis* and the

92 B73 reference maize genome. In some cases, mutations in genes located within those
93 genomic regions result in phenotypes that reveal their involvement in domestication traits.
94 One of the major genes affected by maize domestication is *Teosinte branched1* (*Tb1*), a
95 transcription factor of the TCP family that controls lateral branching, sexual determination,
96 and glume formation (Doebley et al. 1997; Martín-Trillo and Cubas 2010). *Tb1* acts as a
97 repressor of lateral branching (Studer et al. 2017), giving rise to maize plants usually
98 composed of a single stem. Other genes involved in domestication include *Teosinte glume*
99 *architecture1 (Tga1)*, *ramosa2 (ra2)* and *Zea floricaula leafy2 (zfl2),* among others
100 (Bomblies and Doebley 2006; Sigmon and Vollbrecht 2010; Wang et al. 2015).
101
102 The importance of phenotypic plasticity is considered as likely relevant in the
103 domestication history of crops (Ross-Ibarra et al. 2007; Lorant et al. 2020; Mueller et al.,
104 2023); however, the role of environmental factors influencing their origins remains elusive
105 and poorly investigated. A previous study showed that teosinte *parviglumis* grown under
106 low temperatures and CO_2 concentrations - reminiscent of those prevailing in the late
107 Pleistocene and early Holocene - exhibit some phenotypes related to the domestication
108 syndrome, including short branches, a single main stalk, and partially open seed fruitcases
109 (Piperno et al. 2015; Piperno et al. 2019); however, the genetic basis of these changes have
110 not been investigated. Although these results suggest that phenotypic plasticity could have
111 influenced the domestication process, to this date there are no hints on how the adaptation
112 to local environmental conditions could have affected specific gene function and guided
113 human selection.
114
115 Recent genomic evidence indicates that admixture of maize with native teosinte *mexicana*
116 populations (*Zea mays* ssp. *mexicana*) contributed to maize adaptation across a wide range
117 of altitudes and latitudes in the American continent (Yang et al. 2023); however, the earliest
118 maize macro-specimens found to date lack teosinte *mexicana* admixture and exhibit
119 morphological attributes of fully domesticated cobs, indicating that *mexicana* is not a direct
120 ancestor of maize and that its introgression occurred after initial divergence from teosinte
121 *parviglumis* (Vallebueno-Estrada et al. 2023; Acosta-Bayona et al. 2024). Consequently,
122 the nature of the genetic factors that guided the emergence of maize remain largely

123 unknown, and the initial phenotypic changes that caused the original divergence of these
124 two subspecies have not been identified. It is also unknown if domestication initiated by
125 direct action of human selection on teosinte natural standing variation, or if the response to
126 specific environmental factors generated phenotypic changes that were identified and
127 selected by humans to act on native teosinte *parviglumis* populations.
128
129 Maize can adapt to abiotic factors such as heavy metal (HM) stress through numerous
130 mechanisms that prevail during development (AbdElgawad et al. 2020; Gallo-Franco et
131 al. 2020; Malenica et al. 2021; Gao et al. 2022). These include metal immobilization by
132 mycorrhizal association, metal sequestration, or complexation by exuding organic
133 compounds from roots, metal intracellular sequestration and compartmentalization in
134 vacuoles. HMs include essential elements that are necessary for maize growth through
135 enzymatic function, such as iron (Fe), manganese (Mn), zinc (Zn), magnesium (Mg),
136 molybdenum (Mo), and copper (Cu); and non-essential elements like Cadmium (Cd),
137 chromium (Cr), lead (Pb), aluminum (Al), and selenium (Se). In general, HM stress leads
138 to visibly reduced plant growth due to the reduced cell elongation and cell wall elasticity.
139 At the molecular level, metal toxicity can disturb the cellular redox balance and lead
140 directly or indirectly to oxidative stress and the formation of reactive oxygen species
141 (ROS), shifting the redox balance to the pro-oxidative side until the antioxidative defense
142 system allows a new balanced redox status (Smeets et al. 2009; Hall 2002).
143
144 The comparison of the *Palomero toluqueño* and B73 genomes resulted in the identification
145 of a large collection of identical sequence regions (IdSRs) with low nucleotide variability
146 and transcriptional evidence of expression (Vielle-Calzada et al. 2009). Putative
147 domestication loci included *ZmHMA1* and *ZmHMA7*, two genes encoding members of the
148 $P1_b$-ATPases protein superfamily, also known as Heavy Metal ATPases (P-type ATPases)
149 characterized by the generation of a phosphorylated intermediate during the transport
150 reaction cycle. Members of this superfamily contain 8 to 12 transmembrane domains as
151 well as conserved ATP binding, phosphorylation and dephosphorylation sites (Solioz and
152 Vulpe 1996; Axelsen and Palmgren 2001; Voskoboinik et al. 2003; Williams and Mills
153 2005). The superfamily can be divided in subfamilies that include H±ATPases (type 3_A) in

154 plants and fungi, Na+/K ATPases (type $2_{C/D}$) in animals, Ca2±ATPases (type $2_{A/B}$), and
155 heavy metal (HM) transporting ATPases (type 1_B) capable of transporting a large variety
156 of HM cations across cell membranes. *ZmHMA1* and *ZmHMA7* are type 1_B ATPases that
157 include a conserved Cys-Pro-Cys/His/Ser motif within a transmembrane domain necessary
158 for the translocation of HMs cations through the membrane channel. A third *Palomero*
159 *toluqueño*/B73 IdSR included *Skewed Root Growth Similar5* (*ZmSKUs5*), a gene encoding
160 a Skewed5 (SKU5)-similar (SKS) protein classified as a multi-copper oxidase containing
161 cuperdoxin domains (Sedbrook et al. 2002). All three genes map to chromosome five
162 (chr.5), with *ZmHMA1* and *ZmSKUs5* within a genomic region that fractionates into
163 multiple QTLs under selection during the *parviglumis* to maize transition (Doebley and
164 Stec 1993; Lemmon and Doebley, 2014). Contrary to major domestication loci showing a
165 single highly pleiotropic gene responsible for important domestication traits, in this chr.5
166 genomic region the smallest 1.5-LOD support interval contained more than 50 genes,
167 suggesting that phenotypic effects are due to multiple linked QTLs (Lemmon and Doebley,
168 2014). While the functional characterization of all three maize genes remains elusive, the
169 Arabidopsis and barley *ZmHMA1* homologs act during heavy metal transport in the
170 chloroplast (Boutigny et al. 2014), demonstrating their functional involvement in
171 homeostasis.
172
173 To investigate the possibility that HM response had an effect on the origin and
174 domestication of maize, we compared the phenotypic changes that teosinte *parviglumis*
175 and maize undergo when grown in the presence of sublethal concentrations of Cu and Cd.
176 We show for the first time that teosinte *parviglumis* responds to HM stress by acquiring an
177 aerial architecture reminiscent of extant maize and unusual proliferation of female
178 inflorescences. *Tb1* expression is upregulated in teosinte *parviglumis* meristems when
179 grown under HM stress. Analysis of nucleotide variability across 11.46 Mb of chr.5
180 indicates that many genes within the *ZmHMA1 to ZmSKUs5* genomic region show reduced
181 nucleotide variability in maize as compared to teosinte *parviglumis*. Although the reduction
182 is not specific to these genes, large-scale transcriptional analyses suggests that contrary to
183 genes involved in other types of abiotic stress, a large number of loci that contain HM
184 response genes were affected by positive selection during the teosinte *parviglumis* to maize

185 transition. Both *ZmHMA1* and *ZmHMA7* are active throughout maize and teosinte
186 *parviglumis* development, and their expression responds to HM stress. In addition,
187 mutations in *ZmHMA1* show domestication-related defects such as the absence of seminal
188 roots and increased height, both manifested under exposure to HMs. Paleoenvironmental
189 studies reveal a temporal and geographical convergence that relates the history of volcanic
190 eruptions in the TMVB with the emergence of maize at times of climatic instability.
191 Overall, this evidence indicates that the evolutionary transition that gave rise to extant
192 maize was influenced by heavy metal stress through the activity of P1b-ATPases,
193 presumably responding to edaphological consequences of volcanic activity.
194

195 **Results**

196

197 ***Teosinte parviglumis responds to heavy metal stress by acquiring an architecture***
198 ***reminiscent of extant maize.***

199

200 To compare HM response in teosinte *parviglumis* and maize, we exposed wild-type W22
201 maize inbred and CIMMYTMA 29791 teosinte *parviglumis* individuals to sublethal
202 concentrations of Cu (400 mg/kg of $CuSO_4$) and Cd (16mg/kg of $CdCl_2$). $CuSO_4$ and $CdCl_2$
203 were homogenized in soil before transplant and grown under controlled greenhouse
204 conditions. HM concentrations were based on preliminary dose responses that allowed
205 maize plants to reach reproductive stages and complete their life cycle (AbdElgawad et al.
206 2020). Whereas higher doses impair flowering or are lethal, lower Cu/Cd concentrations
207 do not consistently show conventional phenotypic responses such as reduced plant growth
208 (AbdElgawad et al. 2020; Atta et al., 2023). As previously reported (Atta et al. 2023),
209 maize individuals grown in the presence of HMs showed a significant reduction in aerial
210 traits such as stem diameter, size of leaves, size and number of roots, and size of female
211 inflorescences (Figure 1; Tables 1 and S1). On average, stem diameter showed a significant
212 reduction of about 17% ($P<0.05$) as compared to plants grown in absence of HM stress
213 (Figure 1f to 1j). Similarly, the length and width of developing leaves showed significant
214 reductions of 12%, and mature leaves of 6% ($P<0.05$). Reproductive traits such as the
215 number of female inflorescences (NFI) and their average weight (WFI) showed reductions,

216 as previously reported (NFI = 1.20 ± 0.42 in absence of HMs and NFI = 0.70 ± 0.67 in
217 presence of HMs; WFI = 40.06 ± 14.39 in absence of HMs and WFI = 37.75 ± 18.83 in
218 presence of HMs; Table 1). However, the most significant effects occurred in the root
219 system, with an increase in the number of brace roots under HMs (NBR = 12.90 ± 4.33 in
220 absence of HMs; NBR = 16.30 ± 4.99 in presence of HMs; Table 2), and a significant
221 decrease in their length (LBR = 16.15 ± 9.75 cm in absence of HMs; LBR = 4.00 ± 2.04
222 cm in presence of HMs; P<0.001; Table 1). The number and length of crown roots were
223 reduced on average by 33% and 18%, respectively (NCR = 11.30 ± 2.11 in absence of
224 HMs; NCR = 7.60 ± 0.97 in presence of HMs; LCR = 58.90 ± 21.87 cm in absence of
225 HMs; LCR = 48.85 ± 11.80 cm in presence of HMs; Table 1). Nodal roots also showed a
226 significant reduction in their number and length (P<0.01 and P<0.001, respectively; NNR
227 = 10.50 ± 2.27 in absence of HMs; NNR = 6.70 ± 2.79 in presence of HMs; LNR = 87.20
228 ± 16.80 cm in absence of HMs; LNR = 55.30 ± 21.10 cm in presence of HMs; Table 1).
229 By contrast, the number (NSR) and length (LSR) of seminal roots was significantly
230 increased in the presence of HMs (P<0.001 and P<0.01, respectively: NSR = 4.10 ± 1.45
231 in absence of HMs; NSR = 6.60 ± 1.35 in presence of HMs; LSR = 27.70 ± 13.38 cm in
232 absence of HMs; LSR = 43.50 ± 14.01 cm in presence of HMs) when measured 50 days
233 after transplant (Table 1).
234
235 Interestingly, teosinte *parviglumis* exhibited a maize-like phenotype when grown in the
236 presence of HMs, with complete absence of tillering in most plants (Figure 1; Tables 2, S1
237 to S3). This phenotype had never been reported for teosinte *parviglumis* plants grown under
238 HM stress or any other type of edaphological conditions. From a total of 30 plants tested,
239 28 showed total absence of tillering, and two initiated secondary stems during vegetative
240 stages but arrested their growth early during development, resulting in the presence of a
241 single stem at reproductive stages (Figure 1a to 1d; and Table 2). Additionally, all 30 plants
242 tested showed complete absence or residual lateral branching with unusual proliferation of
243 female inflorescences arising from independent axillary meristems in primary stems
244 (Figure 1e). This additional phenotype had not been reported for teosinte *parviglumis* under
245 any type of environmental conditions. The increase in the number of female inflorescences
246 clustered within a single stem (NFI = 1.80 ± 0.63 in absence of HMs; NFI = 3.90 ± 1.66 in

247 presence of HMs; Figure 1e and Table 2) was associated with shorter flowering time as
248 compared with normal growing conditions in absence of HMs (Figure 1d). In addition,
249 teosinte *parviglumis* grown in the presence of HMs showed reduced leaf length (LIL =
250 71.30 ± 11.32 cm in absence of HMs; 56.25 ± 7.80 cm in presence of HMs; Table 2). The
251 absence of lateral branches resulted in lower values of aerial dry weight (DWAP = 133.49
252 ± 28.28 gr in the absence of HMs; DWAP = 82.72 ± 11.67 gr in presence of HMs; Table
253 2). Teosinte *parviglumis* grown under HMs showed a significant reduction in the length of
254 brace roots (P<0.01; LBR = 20.00 ± 11.49 cm in absence of HMs; LBR = 2.88 ± 0.66 cm
255 in presence of HMs; Table 2), but no significant changes in their number. The number
256 crown and nodal roots was significantly decreased by HM stress (P<0.001 and P<0.01
257 respectively; NCR=12.88 ± 4.34 in absence of HMs; 9.6 ± 1.43 in presence of HMs;
258 NNR=16.2 ± 4.69 in absence of HMs; NNR= 14 ± 3.2 in presence of HMs; Table 2). By
259 contrast, the length of nodal roots was significantly increased by HM stress (P<0.001;
260 LNR=83 ± 15.76 in absence of HMs; 104 ± 8.46 in presence of HMs). The presence of
261 HMs did not modify the absence of seminal roots intrinsic to teosinte *parviglumis*
262 accessions (Perkins and Lynch 2021). Taken together, these results suggest that the
263 response of maize and teosinte *parviglumis* to HM stress can give rise to phenotypes
264 previously shown to distinguish both subspecies at the light of the domestication syndrome.
265
266
267 ***Genomic regions encompassing ZmHMA1, ZmHMA7 and ZmSKUs5 show reduced***
268 ***nucleotide variability in extant maize as compared to teosinte parviglumis.***
269
270 *ZmHMA1* and *ZmSKU5* mapped 52.1 and 41.8 cM, respectively, in a genetic map of chr.5
271 calculated to be 86.64 cM, with an average megabase pair to centimorgan ratio of 1.873
272 Mbp/cM (Lemmon and Doebley, 2014; Figure S1). The corresponding mapping population
273 used isogenic recombinant inbred lines (NIRILs) with informative cross-over events
274 concentrated in the region of interest and replicated phenotypic assessments in block
275 experiments. Multiple QTLs were detected in a region spanning across 82 cM, none with
276 single large effect genes such as those found in other chromosomes (Wang et al., 2005;
277 Studer et al. 2011; Wills et al., 2013), suggesting that several associated domestication

278 traits are due to multiple linked QTLs of small effect (Lemmon and Doebley, 2014). The
279 location of *ZmSKU5* overlaps with a single wide 1.5-LOD support interval that spreads
280 across 50.6 cM (number of kernels per rank; Figure S1). By contrast, *ZmHMA1* overlaps
281 with a contiguous region containing no less than five QTL 1.5- LOD support intervals (ear
282 diameter; number of kernels per rank; percentage of staminate spikelets; tassel branch
283 number; and tillering index; Figure S1).
284
285 To determine if the regulatory and coding regions of *ZmHMA1, ZmHMA7,* and *ZmSKUs5*
286 were affected by human selection, we calculated their level of nucleotide variability based
287 on single nucleotide polymorphisms (SNPs) for all extant maize and teosinte *parviglumis*
288 accessions included in the diversity panel HapMap3, using the corresponding sequences of
289 *Tripsacum dactyloides* as an outgroup. The levels of the nucleotide variability index - π(m)
290 and π(t) for maize and teosinte *parviglumis*, respectively - were determined in bins of 100
291 nt using VCFtools, including alignments encompassing a genomic region that included 15
292 kb upstream of the START codon, the corresponding coding region for each gene, and 15
293 kb downstream of the STOP codon (Figure 2 and Table S4). In the case of *ZmHMA1*, the
294 upstream region values were π(m)= 0.00071 and π(t)= 0.00870, and for the downstream
295 region, π(m)=0.00097 and π(t)=0.00248. By contrast, the *ZmHMA1* coding sequence
296 showed low values in both subspecies: π(m)= 0.0050 and π(t)= 0.00106. These results
297 indicate that human selection in the *ZmHMA1* locus preferentially affected its upstream
298 and downstream regulatory regions (Figure 2a and Table S4). *ZmHMA7* showed
299 contrasting values of π(m) and π(t) across the entire coding sequence and its regulatory
300 regions (Figure 2b). For the upstream region, values were π(m)= 0.0009 and π(t)=0.00411;
301 for the *ZmHMA7* coding region, π(m)= 0.00015 and π(t)= 0.00148; and for the downstream
302 region, π(m)=0.00066 and π(t)=0.00454. *ZmSKUs5* also showed contrasting nucleotide
303 variability in the entire coding and flanking regions (Figure 2c and Table S4). Values were
304 π(m)= 0.0011 and π(t)= 0.00735 for the upstream region, π(m)= 0.00044 and π(t)= 0.00754
305 for the coding sequence, and π(m)=0.00203 and π(t)=0.00626 for the downstream region
306 (Table S4). For all three genes, similar π values in the coding region of maize landraces
307 and improved lines indicates that the loss of nucleotide variability occurred during the
308 teosinte *parviglumis* to maize transition, and not during subsequent contemporary breeding

309 (Table S4). By contrast, the *ZmGLB*1 neutral control locus shows equivalent levels of
310 nucleotide variability in maize and teosinte *parviglumis* (Eyre-Walker et al. 1998).
311
312 We also compared the level of genetic variability in *ZmHMA1*, *ZmSKUs5*, and *ZmHMA7*
313 (and their neighboring regions) to all chr.5 genes categorized as likely affected by
314 domestication (Hufford et al., 2012), and to the full collection of neutral genes distributed
315 across the whole chromosome. The analysis was conducted using 100 bp bins and sliding
316 windows of 50 bp; for a total of 385,829 bins in the case of chr.5 domestication genes, and
317 2,373,010 bins for neutral genes. As shown in Figure S2, the levels of nucleotide variability in
318 the three candidate genes and their six neighboring loci are significantly reduced in maize
319 landraces as compared to teosinte *parviglumis* inbred lines. When compared to the full neutral
320 gene set of chr.5, this reduction is more severe than the reduction affecting 304 previously
321 identified domestication genes, confirming the exceptional selective pressure that was imposed
322 in those three loci during the evolutionary transition from teosinte *parviglumis* to extant
323 maize.
324
325 ***Large-scale genomic and transcriptomic comparisons indicate that many HM response***
326 ***genes were positively selected across the maize genome.***
327
328 To expand the results well beyond the analysis of the three genes previously described, we
329 performed a detailed analysis of genetic diversity across the 11.47 Mb genomic region
330 comprised between *ZmSKUs5* and *ZmHMA1*. This additional analysis reveals general
331 tendencies in the quantity and nature of loci that were affected by positive selection during
332 the teosinte *parviglumis* to maize transition in region identified via LOD score on chr.5.
333 We compared nucleotide variability by using 100 bp bins covering loci composed of two
334 30 Kb segments up and downstream of coding sequences, respectively, and the coding
335 sequence itself, for 173 genes present within the genomic region comprised between
336 *ZmSKUs5* and *ZmHMA* (Figure S1 and Supplementary File 6). Two types of statistical tests
337 (ANOVA and Wilcoxon) were applied to nucleotide variability comparisons using the
338 entirety of each locus. The Benjamini-Hochber procedure allowed an estimation of the
339 false discovery rate (FDR<0.05) to avoid type I errors (false positives). Although some
340 individual loci appear as differently classified depending on the statistical test applied (22

341 out of 173 loci), the general differences in nucleotide variability are consistently
342 maintained within the subregions described below. We found that 166 out of 173 loci show
343 signatures of positive selection and are roughly organized in five independent subregions
344 of variable length. The first six loci are consecutively ordered in a 402 Kb subregion that
345 includes *ZmSKUs5.* A second group of 13 consecutive loci expands over a 1.44 Mb
346 subregion that contains *NRAMP ALUMINUM TRANSPORTER1*, also involved in HM
347 response through uptake of divalent ions. A third group of 17 consecutive loci expands
348 over 1.28 Mb; eleven contain genes encoding for uncharacterized proteins. The fourth
349 group is composed of 57 consecutive loci expanding over 3.22 Mb and contains genes
350 encoding for *DEFECTIVE KERNEL55, AUXIN RESPONSE FACTOR16*, and peroxydases
351 involved in responses to oxydative stress. The fifth group contains 12 consecutive loci
352 expanding over 713 Kb and contains *ZmHMA1.* An additional segment of approximately
353 1.17 Mb and containing 25 consecutive loci that were positively selected expands away
354 from the *ZmSKUs5-ZmHMA1* segment; it also contains several genes encoding for
355 peroxydases. Although multiple loci include genes that could be involved in abiotic stress
356 and oxidative responses, these results suggest that multiple factors other than HM stress
357 could have played a role in the evolutionary mechanisms that affected the genetic diversity
358 of chr.5 during the teosinte *parviglumis* to maize transition.
359
360 To further analyze the possibility that HM response could have played a role in maize
361 emergence and subsequent domestication, we analyzed large scale transcriptomic data
362 corresponding to independent experiments aiming at understanding the response of maize
363 roots to HM stress. Six available transcriptomes were selected for in-depth analysis because
364 they presented a fold change strictly higher than 1, and their results were supported by false
365 discovery rates (FDR<0.05). These six transcriptomes (Table S5) included HM response
366 datasets corresponding to growth conditions that not only incorporated Cu, but also lead
367 (Pb) and chromium (Cr) that were not included in the substrate of our experiments.
368 Transcriptional profiles were obtained from roots of plants at different stages: maize
369 seedlings (Shen et al., 2012; Gao et al., 2015; Zhang et al., 2024a), three week old plantlets
370 (Yang et al., 2023), and plants at V2 stage (Zhang et al., 2024b; Fengxia et al., 2025). A
371 total of 120 genes shared by all six transcriptomes were found to be differentially expressed

372 under HM stress conditions (66 upegulated and 54 downregulated; Figure S3), including
373 *ZmSKUs5*, *ZmHMA1* and *ZmHMA7*; 52 of them (43.3%) are located in maize loci showing
374 less than 70% of the nucleotide variability found in teosinte *parviglumis*, suggesting that
375 they were affected by positive selection (Yamasaki et al., 2005; Supplementary File 7). Of
376 18 mapping in chr.5, twelve are within the 82 cM that fractionates into multiple QTLs
377 under selection during the *parviglumis* to maize transition. Interestingly, five additional
378 loci containing HM response genes completely lack SNPs within their total length in both
379 *parviglumis* and maize, and 19 additional loci lack SNPs in at least one 30 Kb segment or
380 their coding region (Supplementary File 7), suggesting the frequent presence of
381 ultraconserved genomic regions in many loci containing HM response genes. When this
382 same analysis was conducted in a set of loci comprising 63 genes previously identified as
383 differentially expressed in response to abiotic stress not directly related to HM responses
384 (hypoxia; nutritional deficiency; soil alkalinity; drought; soil salinity), 18 loci (28.6%)
385 showed less than 70% of the nucleotide variability found in teosinte *parviglumis*. Only one
386 of them maps in chr.5 and none contained segments or coding regions lacking SNPs in
387 *parviglumis* or maize. These results suggest that in contrast to other types of abiotic stress
388 response genes, loci comprising a large set of genes that unambiguously respond to HM
389 stress caused by chemical elements of diverse nature were affected by positive selection
390 during the *parviglumis* to maize transition, irrespectively of their position in the genome.
391
392
393 ***ZmHMA1 and ZmHMA7 are active throughout development and their expression is***
394 ***influenced by the presence of heavy metals.***
395
396 The gene structure of *ZmHMA1, ZmHMA7,* and *ZmSKUs5* is shown in Figure 3. The coding
397 sequence of *ZmHMA1* and *ZmHMA7* is approximately 21.6 Kb and 4.5 Kb, respectively,
398 while *ZmSKUs5* is approximately 4.2 Kb in length. Within the short arm of chromosome
399 5, *ZmHMA1* and *ZmSKUs5* are separated by 9.16 Mb, with *ZmHMA1* approximately 15
400 Mb away from the maximum likelihood prediction of a QTL involved in maize
401 domestication (Doebley and Stec 1993; Vielle-Calzada et al. 2009). *ZmHMA7* maps to the
402 centromeric region of chromosome 5. A detailed PlantCARE-based analysis identified

403 several conserved binding sites and regulatory elements in the promoter region of these
404 three genes (Lescot et al. 2002). *ZmHMA1* and *ZmHMA7* share binding sites to basic Helix-
405 Loop-Helix (bHLH) transcription factors, as well as abscisic acid response (ABRE),
406 ethylene responsive (ERF), and G-box (CACGTG) elements recognized by leucine zipper
407 family (bZIP) and bHLH transcription factors (Figure 3a). The regulatory region of both
408 *ZmHMA1* and *ZmSKUs5* contain a binding site for MIKC-type MADS box transcription
409 factors (Figure 3a), whereas *ZmHMA7* and *ZmSKUs5* share a jasmonic acid-response
410 TGACG-motif (Figure 3a), as well as a Myb-binding (MBS) and GATA binding site. In
411 addition, *ZmHMA1* contains a binding site for TCP proteins such as Tb1, increasing the
412 number of families of transcription factors that could be involved in shared or individual
413 regulation of these three genes (Figure 3a).
414
415 To elucidate the expression patterns of *ZmHMA1* and *ZmHMA7*, we conducted reverse
416 transcriptase PCR (RT-PCR) in leaves, stems, roots, and flowers at two vegetative (V2 and
417 V6) and one reproductive (R1) developmental stage, in teosinte *parviglumis* and wild-type
418 W22 maize individuals (Figure 3b). In the case of maize, *ZmHMA1* was expressed in
419 leaves, stems, roots and flowers throughout development in either absence or presence of
420 HMs. *ZmHMA7* was also expressed in aerial organs throughout development in both
421 absence and presence of HMs but was not expressed in roots at reproductive stage R1. In
422 teosinte *parviglumis, ZmHMA1* was also expressed throughout development in either
423 absence or presence of HMs. By contrast, ZmHMA*7* was constitutively expressed in aerial
424 organs, but only expressed in roots under HM stress during V2 and V6 stages. To further
425 determine if the level of expression of these two genes is influenced by the presence of
426 HMs, we conducted quantitative real-time PCR (qPCR) using the primary root of teosinte
427 *parviglumis* and maize plantlets at four weeks after germination (Figures 3c and 3d). In
428 wild-type W22 maize, the expression of *ZmHMA1* was not significantly different in the
429 presence and absence of HMs. By contrast, in teosinte *parviglumis* the expression of
430 *ZMHMA1* was significantly increased in presence of HMs (Figure 3c). In the case of
431 *ZmHMA7*, expression was significantly increased in both maize and teosinte *parviglumis*
432 when plants were grown in the presence of HMs (Figure 3d). Overall, these results indicate

433 that the activity of both *ZmHMA1* and *ZmHMA7* is influenced by HM stress in teosinte
434 *parviglumis* and maize.
435
436
437 ***ZmHMA1 null mutant individuals show phenotypic defects related to the domestication***
438 ***syndrome.***
439
440 Transposon *Mu* insertional lines have been widely used to elucidate gene function in maize.
441 To elucidate the function of *ZmHMA1*, we phenotypically analyzed *LANMu1029790*, a 4-
442 generation backcross of line *mu1029790* into the W22 background selected for single copy
443 insertions in *ZmHMA1* (McCarty et al. 2005). In *LANMu1029790,* a single *Mu* insertion is
444 in the first exon of *ZmHMA1*, 65 bp downstream of the START codon (Figure 3a). RT-
445 PCR analysis showed that expression of Z*mHMA1* is completely absent in homozygous
446 individuals for the *LANMu1029790* insertion (Figure S4), confirming that the
447 corresponding mutant is a null allele. Plants harboring a homozygous *LANMu1029790*
448 insertion are subsequently designated as *zmhma1-m1::MuDR* (abbreviated *zmhma1-m1*).
449
450 To determine the function of *ZmHMA1* in maize, we compared the phenotype of wild-type
451 W22 and homozygous *zmhma1-m1* individuals at the reproductive R1 stage (Table 1).
452 Under normal growing conditions, homozygous *zmhma1-m1* individuals generated
453 significantly less leaves than wild-type ($P<0.001$; NL = 13.4 ± 0.84 in wild-type, and NL
454 = 11.4 ± 0.84 in *zmhma1-m1*). Whereas the length of mutant leaves was smaller than wild-
455 type (LML = 77.4 ± 6.64 cm in wild-type, and LML = 69.85 ± 9.18 cm in *zmhma1-m1*),
456 their width was significantly larger ($P<0.001$; WML = 6.75 ± 1.3 cm in wild-type, and
457 WML = 9.75 ± 1.4 cm in *zmhma1-m1*), resulting in an increase of the total dry weight of
458 aerial organs in mutant plants (DWAP = 18.43 ± 8.04 grams in wild-type, and DWAP =
459 28.46 ± 9.54 grams in *zmhma1-m1*). Homozygous *zmhma1-m1* individuals also produced
460 significantly more female inflorescences per plant ($P<0.001$; NFI = 1.2 ± 0.42 in wild-type,
461 and NFI = 1.9 ± 0.32 in *zmhma1*) a difference that reflected in the total dry weight of female
462 inflorescences per plant ($P<0.001$; WFI = 40.06 ± 14.39 gr in wild-type and WFI = 69.5 ±
463 11.2 gr in *zmhma1*); and significantly more spikes per male inflorescence ($P<0.001$; NSB

464 = 9 ± 1.63 in wild-type, and NSB = 13.4 ± 2.32 in *zmhma1-m1*). Interestingly, the general
465 length of roots was significantly smaller in homozygous *zmhma1-m1* individuals, in
466 particular nodal roots (P<0.001; LNR = 87.2 ± 16.8 cm in wild-type, and LNR = 50.9 ±
467 12.83 cm in *zmhma1-m1*). By contrast, mutant plants showed a significant increase in the
468 number of seminal roots per plant (P<0.001; NSR = 4.1 ± 1.45 in wild-type, and NSR =
469 7.3 ± 1.16 in *zmhma1-m1*). When wild-type and mutant individuals were grown under HM
470 stress, differences in the size of leaves, number of female inflorescences per plant, and
471 number of spikes per male inflorescence were maintained. In addition, mutant individuals
472 exposed to HM stress were significantly taller than wild-type (P<0.01; HEI = 82.2 ± 34.94
473 cm in wild-type, and HEI = 125.9 ± 18.81 cm in *zmhma1-m1*). In addition, total root and
474 seminal root length were equivalent in wild-type and mutant individuals, mainly because
475 the length of wild-type roots was significantly reduced under HM stress; however, the
476 number of seminal roots was again significantly higher in mutant individuals (P<0.05; NSR
477 = 6.6 ± 1.35 in wild-type, and NSR = 8.2 ± 1.62 in *zmhma1-m1*). These results indicate
478 that in maize aerial organs, *ZmHMA1* is involved in promoting leaf growth, restricting the
479 number of female inflorescences per plant, and restricting the number of spikes in male
480 inflorescences. In underground organs, *ZmHMA1* is involved in promoting root growth and
481 restricting the number of seminal roots per individual. Under HM stress, *ZmHMA1* shows
482 an additional role in restricting plant height, a function that was not identified under normal
483 growing conditions. Overall, these results suggest that *ZmHMA1* is involved in the control
484 of some of the aerial and underground phenotypic traits that distinguish maize from teosinte
485 *parviglumis,* especially under HM stress conditions.
486
487
488 ***Under heavy metal stress, Tb1 is overexpressed in the apical meristem of teosinte***
489 ***parviglumis.***
490
491 The absence of secondary ramifications in teosinte *parviglumis* grown under HM stress is
492 reminiscent of the aerial architecture of wild-type maize. Previous QTL and molecular
493 analysis suggested that *Tb1* contributed to the architectural difference between maize and
494 teosinte, as *tb1* maize mutants develop secondary stem ramifications ending in male

495 inflorescences, resembling teosinte in their overall architecture (Doebley et al. 1997).
496 Interestingly, the regulatory region of *ZmHMA1* contains a specific binding site for
497 members of the Teosinte-branched 1/Cycloidea/Proliferating (TCP) family of transcription
498 factors that includes Tb1 (Figure 3a). To investigate the possibility that the phenotypic
499 response of teosinte *parviglumis* under HM stress could be regulated by *Tb1*, we conducted
500 quantitative real-time PCR (qPCR) to determine the expression of *ZmHMA1* and *Tb1* in
501 the shoot apical meristem (SAM) of one month old W22 maize and teosinte *parviglumis*
502 plantlets (Figure 4a and 4b). The expression *ZmHMA1* was downregulated in W22 wild-
503 type maize meristems in the presence of HMs. By contrast, HM stress resulted in a
504 significant increase of *ZmHMA1* expression in teosinte *parviglumis*, confirming that in the
505 maize ancestor the level of *ZmHMA1* activity is influenced by the presence of HMs in the
506 soil. In addition, the expression of *Tb1* was significantly upregulated in teosinte
507 *parviglumis* meristems in the presence of HMs. These results do not allow to directly link
508 the regulation of *ZmHMA1* expression to the function of *Tb1*; however, they open an
509 opportunity to further investigate the possibility that under HM stress, the formation of
510 secondary ramifications in teosinte *parviglumis* could be repressed by transcription factors
511 of the TCP family, including Tb1.
512
513
514 ***Paleoenvironmental studies reveal periods of climatic instability in the presumed region***
515 ***of maize emergence during the early Holocene.***
516
517 It is well accepted that temperature fluctuations, volcanism and anthropogenic impact
518 shaped the distribution and abundance of plant species in the Transmexican Volcanic Belt
519 (TMVB) during the last 14,000 years (Torrescano-Valle et al. 2019). The TMVB has
520 produced close to 8000 volcanic structures (Ferrari et al., 2011), transforming the relief
521 multiple times, and causing hydrographic and soil changes that actively modified the
522 distribution and composition of plant communities in Central Mexico. Detailed
523 paleoenvironmental data for the Pleistocene and Holocene is available for several
524 lacustrine zones located within the 50 to 100 km range of the region currently considered
525 the cradle of maize domestication (Matzuoka et al. 2002; Figure 5a). In Lake Zirahuén

(102°44′ W; 19°26′ N and approximately 2075 meters above sea level; index [i] in Figure 5a), pollen, microcharcoal and magnetic susceptibility analyses of two sedimentary sequences reveals three periods of major ecological change during the early and middle Holocene. Between 9500 and 9000 calibrated years before present (cal yr BP), pine forests seem to have been associated with summer insolation increases. A second peak of forest change occurred at around 8200 cal yr BP, coinciding with cold oscillations documented in the North Atlantic. Finally, events occurred between 7500 and 7100 cal yr BP shows an abrupt change in the plant community related to humid Holocene climates and a presumed volcanic event (Lozano-García et al., 2013). The environmental history of the central Balsas watershed has also been documented by pollen, charcoal, and sedimentary analysis conducted in three lakes and a swamp of the Iguala valley (Piperno et al. 2007). Paleoecological records of lake Ixtacyola (8°20N, 99°35W and approximately 720 meters above sea level; index [ii] in Figure 5a) and lake Ixtapa (8°21N, 99°26W) indicate that an important increase in temperature and precipitation occurred between 13000 and 10000 cal yr BP. The pollen record of Ixtacyola showed that members of the genus *Zea* were already part of the vegetation coverage by 12900 to 13000 cal yr BP, suggesting that some teosintes – likely including *parviglumis* - were commonly found at elevation areas where they do not presently occur. Lake Almoloya (also named Chignahuapan; 19°05N, 99°20E and approximately 2575 meters above sea level; index [iii] in Figure 5a) in the upper Lerma basin is only 20 Km from the crater of the Nevado de Toluca that is responsible for creating the late Pleistocene Upper Toluca Pumice layer over which the Lerma basin is deposited. Pollen records indicate the presence of *Zea* species by 11080 to 10780 cal yr BP. As for other locations, an important period of climatic instability prevailed between 11500 and 8500 cal yr BP (Ludlow-Wiechers et al., 2005). Humidity fluctuations occurred until 8000 cal yr BP, with a stable temperate climate between 8500 and 5000 cal yr BP. Although pollen and diatom studies are often difficult to interpret at a regional scale, the overall reported results suggest consistent periods of *Zea* plants present in periods of environmental and climatic instability that correlate with the history of volcanic activity during the early Holocene, as described in the next section.

557
558
559 ***Temporal and geographical convergence between volcanic eruptions and maize***
560 ***emergence during the Holocene.***
561
562 Current evidence indicates that the emergence and domestication of maize initiated in
563 Mesoamerica some time around 9,000 yr BP (Matsuoka et al. 2002). The current location
564 of teosinte *parviglumis* populations that are phylogenetically most closely allied with maize
565 are currently distributed in a region located between the Michoacan-Guanajuato Volcanic
566 Field (MGVF) at their northwest, and the Nevado de Toluca and Popocatéptl volcanoes at
567 their east and northeast (Figure 5a; Matsuoka et al. 2002). Precise records of field data
568 indicate that ten accessions were collected in the Balsas river drainage near Teloloapan and
569 Sierra de Huautla (Guerrero), at approximately 100 km south of the Nevado de Toluca
570 crater (Matzuoka et al. 2002). Three other accessions were collected near Tejupilco de
571 Hidalgo and Zacazonapan (Estado de México), at approximately 50 to 60 km from the
572 Nevado de Toluca crater (8762, JSG y LOS-161, and JSG-391). And four other accessions
573 were located in Michoacan, at a location within the MGVF (accession 8763), or at mid-
574 distance between the MGVF and the Nevado de Toluca crater (accessions JSG y LOS-130,
575 8761, and 8766).
576
577 The most important source of HMs in ancient soils of Mesoamerica is TMBV-dependent
578 volcanic activity through short- and long-term effects related to lava deposits, ores,
579 hydrothermal flow, and ash (Torrescano-Valle et al. 2019). Interestingly, TMVB activity
580 in the center of Mexico was particularly intense during the Holocene, as compared to other
581 regions and time frames (Marcias and Arce, 2019). The Nevado de Toluca volcano
582 produced one of the most powerful eruptions from central Mesoamerica in the Holocene,
583 giving rise to the Upper Toluca Pumice deposit at 12621 to 12025 cal yr BP (Arce et al.,
584 2003; Figure 5b). The pumice fallout blanketed the Lerma and Mexico basins with 40 cm
585 of coarse ash (Bloomfield and Valastro 1977; Arce et al. 2003). A second eruption dated
586 by ^{36}Cl exposure occurred at 9700 cal yr BP (Arce et al. 2003; Figure 5b), and the most
587 recent eruption occurred at 3580 to 3831 cal yr BP (Macías et al. 1997). During the early

588 and middle Holocene, the Popocatéptl volcano produced at least four eruptions dated
589 13037-12060, 10775–9564, 8328-7591, and 6262-5318 cal yr BP (Siebe et al. 1997); three
590 other important eruptions occurred during the late Holocene, between 2713 and 733 cal yr
591 BP (Siebe and Macías, 2006). In addition, the MGFV is a monogenetic volcanic field for
592 which 23 independent eruptions have been documented during the Holocene, 21 of them
593 located towards the southern part of the field, in close proximity to the region harboring
594 some of the teosinte *parviglumis* populations most closely related to maize. Three of these
595 eruptions occurred in the early Holocene (El Huanillo 1130 to 9688 cal yr BP; La Taza
596 10649 to 10300 cal yr BP; Cerro Grande 10173 to 9502 cal yr BP; Figure 5b), and three
597 others during the initial period of the middle Holocene, between 8400 and 7696 cal yr BP
598 (La Mina, Los Caballos, and Cerro Amarillo; Figure 5b). On average, a new volcano forms
599 every ~435 years in the MGFV (Macías and Arce, 2019). No less than 16 other eruptions
600 occurred between 7159 cal yr BP and the present time (Figure 5b). Soils of volcanic origin
601 (andosols) are currently distributed in regions north-west from the Nevado de Toluca and
602 Popocatéptl craters, in close proximity with teosinte *parviglumis* populations most closely
603 related to maize (Figure S5). Although modern distribution of teosinte populations may
604 differ from their distribution around 9000 yr BP, and unknown populations more closely
605 related to maize may yet to be discovered, this data indicates that the date and region where
606 maize emerged is convergent with the dates and locations of several volcanic eruptions
607 occurred during the Holocene in that same region.
608
609
610 **Discussion**
611
612 Although the evolutionary transition from teosinte *parviglumis* to maize resulted in
613 important phenotypic divergence between landraces and their wild progenitor, the
614 relevance of teosinte *parviglumis* phenotypic plasticity and its genetic consequences during
615 domestication remain poorly understood. Our study offers the first evidence showing that
616 a specific environmental factor (HM stress) influenced the teosinte *parviglumis* to maize
617 transition through specific gene function (HM-response ATPases). The comparison of HM
618 responses between both subspecies indicates that teosinte *parviglumis* phenotypically

619 responds to HM stress acquiring phenotypes reminiscent of maize. Low temperatures and
620 low CO_2 concentrations caused a significant decrease in lateral branching but not in
621 tillering. This decrease of lateral branching correlated with a decrease in teosinte seed yield
622 (Piperno et al. 2015). Similar results were reported for *parviglumis* plants grown under low
623 Nitrogen conditions (Gaudin et al. 2011). Our results under HM stress also show an
624 increase in the number of female inflorescences per plant. This HM stress-dependent
625 proliferation of several closely associated female inflorescences in a single teosinte
626 *parviglumis* stem has not been previously reported. Female inflorescences arose from
627 individual axillary meristems in multiple internodes, significantly increasing teosinte
628 *parviglumis* seed yield. Under HM stress, we also show that *Tb1* is overexpressed in the
629 apical meristem of teosinte *parviglumis,* suggesting that formation of secondary
630 ramifications is repressed by *Tb1* function under HM stress, as in extant maize. At this
631 stage we cannot discard the possibility that *Tb1* upregulation in *parviglumis* reflects a more
632 generalized response to abiotic stress; however, the expression *ZmHMA1* is downregulated
633 in W22 wild-type maize meristems in the presence of HMs but upregulated in teosinte
634 *parviglumis* meristems, suggesting that a specific regulatory shift relating HM responses
635 and *ZmHMA1* function occurred during the teosinte *parviglumis* to maize transition.
636
637 We also show that *ZmHMA1*, *ZmHMA7* and *ZmSKUs5* exhibit reduced genetic diversity in
638 extant maize as compared to teosinte *parviglumis*, suggesting that all three loci were
639 affected by the evolutionary transition that gave rise to maize. The maize regulatory region
640 and downstream 3' area of the *ZmHMA1* locus exhibit pronounced reduction in SNPs
641 compared to teosinte *parviglumis* lines, likely affecting the molecular scope of its
642 regulatory proteins, including transcription factors of the TCP family (Martín-Trillo and
643 Cubas 2010). By contrast, *ZmHMA7* and *ZmSKUs5* showed a selective sweep across the
644 entire maize locus. Although loss of genetic diversity is usually the result of human
645 selection during domestication, it can also represent a consequence of natural selective
646 pressures favoring fitness of specific teosinte *parviglumis* allelic variants better adapted to
647 environmental changes and subsequently affected by human selection during the
648 domestication process. This possibility is reflected by widely spread selective sweeps
649 affecting a large portion of chr.5 that contains hundreds of genes showing signatures of

650 positive selection. The analysis of 11.47 Mb covering the *ZmHMA1-ZmSKUs5* segment
651 confirms the presence of large but discrete genomic subregions that were positively
652 selected during the teosinte *parviglumis* to maize transition. Although several contain
653 genes involved in HM response and oxidative stress, the diversity of gene functions does
654 not necessarily favor abiotic stress over other factors that could be at the origin of selective
655 forces affecting these regions. By contrast, a large scale transcriptomic survey indicates
656 that genes consistently responding to HMs (Cu, Cd, Pb and Cr) show signatures of positive
657 selection at unusual high frequencies (43.3%) as compared to loci containing genes
658 responding to other types of abiotic stress (28.6%). Our identification of HM response
659 genes affected by positive selection is far from being exhaustive. Nevertheless, it agrees
660 with the expected effects of a widespread selective sweep caused by environmental
661 changes that influenced the *parviglumis* to maize transition at the genetic level. Of
662 intriguing interest are 24 loci that partially or completely lack SNPs in both teosinte
663 *parviglumis* and maize, suggesting possible genetic bottlenecks occurred before the
664 teosinte to maize transition. Examples of other edaphological factors driving genetic
665 divergence either in the teosintes or maize include local adaptation to phosphorus
666 concentration in *mexicana* and *parviglumis* (Aguirre-Liguori et al. 2019), and fast maize
667 adaptation to changing iron availability through the action of genes involved in its
668 mobilization, uptake, and transport (Benke and Stich 2011). Our results reveal a teosinte
669 *parviglumis* environmental plasticity that could be related to the function of HM response
670 genes positively selected during the teosinte *parviglumis* to maize transition. Previous
671 studies have demonstrated that transposable elements (TEs) contribute to activation of
672 maize genes in response to abiotic stress, affecting up to 20% of the genes upregulated in
673 response to abiotic stress, and as many as 33% of genes that are only expressed in response
674 to stress (Makarevitch et al., 2015). It is therefore possible that the HM response of some
675 specific genes that influenced maize emergence or domestication could be mediated by
676 TEs influencing or driving their transcriptional regulation.
677
678 The maize genome contains 12 genes encoding for members of the P1b family of ATPases
679 (Cao et al. 2019). They are subdivided according to their preferential substrate affinity: the
680 Copper (Cu)/Silver (Ag) group includes *ZmHMA1* to *ZmHMA4*; and the Zinc (Zn)/Cobalt

681 (Co)/Cadmium (Cd)/Lead (Pb) includes *ZmHMA5* to *ZmHMA12*. Initial studies suggested
682 that *ZmHMA1* is expressed at low levels in vegetative, reproductive or root organs
683 throughout development, contrary to *ZmHMA7* that is strongly expressed in developing
684 seeds 10 days after pollination; however, both genes appeared downregulated in plants
685 grown under either Cu or Cd stress (Zhiguo et al. 2018). Additional studies by Cao et al
686 (2019) indicated low expression of *ZmHMA1* and high levels of *ZmHMA7* expression in
687 12 tissues: roots, nodes, shoots, leaves, tassel, shoot apical meristem and young stem,
688 internodes, anthers, silks, whole seedlings, endosperm, embryo, and pericarp. Under Cd
689 stress, expression of both *ZmHMA1* and *ZmHMA7* was significantly upregulated in roots
690 and downregulated in stems (Cao et al. 2019), contradicting previous results by Zhiguo et
691 al. (2018). In Arabidopsis and barley, the corresponding *ZmHMA1* structural homologs
692 (*AtHMA1* and *HvHMA1*, respectively) can transport a wide range of metals into the
693 chloroplast (Mikkelsen et al. 2012; Boutigny et al. 2014). In the case of the Arabidopsis
694 structural homolog of ZmHMA7, AtHMA7 (also called RAN1) is proposed to act as a
695 metallochaperone located in the Golgi apparatus, delivering Cu to the ethylene receptor
696 located in the plasma membrane (Hirayama et al. 1999). Our evidence complements
697 previous studies by showing that in maize, *ZmHMA1* root expression is restricted to
698 vegetative developmental stages, and that *ZmHMA7* is expressed in roots in response to
699 HM stress. We also show through qPCR analysis that under HM stress, the expression of
700 both *ZmHMA1* and *ZmHMA7* is upregulated in teosinte *parviglumis* primary roots of 4-
701 week-old plantlets. Overall, these results confirm that both *ZmHMA1* and *ZmHMA7* are
702 HM response genes active throughout teosinte and maize development.
703
704 In maize, the phenotypic analysis of null mutant individuals indicates that *ZmHMA1* is
705 involved in the control of aerial and underground developmental traits, some of which are
706 related to important functional adaptations that distinguish maize from its wild ancestor. In
707 addition to changes in leaf number, leaf length, and number of spikes per male
708 inflorescence, *zmhma1-m1* mutant individuals grown under normal edaphological
709 conditions showed an increase in the number of female inflorescences per plant, a reduction
710 in the length of nodal roots, and an increase in the number of seminal roots per plant.
711 Whereas the promotion of nodal root growth is a distinctive trait of maize phenotypic

712 plasticity and adaptation, previous studies showed that contrary to maize, plants of teosinte
713 *parviglumis* lack seminal roots. This absence is also characteristic of paleobotanical maize
714 specimens dating more than 5,000 cal yr BP, confirming that the acquisition of seminal
715 roots is an important trait acquired during domestication (Lopez-Valdivia et al. 2022). The
716 presence of seminal roots distinguishes extant maize from the teosintes (Burton et al. 2013),
717 suggesting a possible involvement in domestication (Perkins and Lynch 2021; Lopez-
718 Valdivia et al. 2022). Our results suggest that the allelic variants of the *ZmHMA1* locus
719 selected during domestication could have contributed to promote seminal root formation
720 in maize, optimizing their number in accordance to seed endosperm availability and
721 carbohydrate reserves (Perkins and Lynch 2021; Lopez-Valdivia et al. 2022). Interestingly,
722 *ZmHMA1* plays an important role in contributing to restricting plant height in response to
723 HM stress, a phenotype that is also an important distinction between teosinte *parviglumis*
724 and maize. Taken together, these results indicate that *ZmHMA1* function was involved in
725 the phenotypic transition from teosinte *parviglumis* to maize through the influence of HM
726 stress; however, a better definition of its role in the origin and domestication of maize will
727 require a functional analysis of the *ZmHMA1* teosinte *parviglumis* homolog, and a detailed
728 molecular analysis of the corresponding allelic variants and their phenotypic effects in both
729 subspecies.
730
731 ***Ideas and Speculation.***
732
733 Our results point to an evolutionary model in which environmental changes in the form of
734 edaphological HM stress imposed natural selective forces that acted on native teosinte
735 *parviglumis* populations, causing phenotypic responses and a severe genetic bottleneck
736 (Figure S6). Adapted plants developed phenotypic traits such as shorter height and
737 emergence of seminal roots, progressively giving raise to primitive maize individuals with
738 reduced genetic variation in HM response genes such as *ZmHMA1*. The subsequent action
739 of human selection caused a drastic reduction in allelic variation of HM response genes,
740 and genetic fixation of the resulting domestication traits.

741

742 The history of eruptive activity in the TMVB during the early Holocene coincides with the
743 temporal estimation of initial stages in the evolutionary transition that gave rise to maize.
744 Intense and recurrent eruptions occurred 12,000 to 6,000 years ago near the region
745 presumed to be the cradle of maize domestication (Matsuoka et al. 2002; Macias and Arce,
746 2019). Located less than 60 Km from the region that harbors some of the natural teosinte
747 *parviglumis* populations most closely related to maize (Matsuoka et al. 2002), the Nevado
748 de Toluca volcano underwent three major eruptions approximately 12621-12025, 9700,
749 and 3580- 3831 yr BP (Macias and Arce, 2019). The large 9700 yr BP eruption caused in
750 the region a period of climatic instability that lasted until 8500 yr BP (Ludlow-Wiechers et
751 al., 2005). Could volcanic eruptions during the early Holocene have modified soil
752 composition and influence the initial evolutionary transition from teosinte *parviglumis* to
753 primitive maize? The possibility of environmental cues influencing maize emergence was
754 mentioned by Benz and Iltis (1992), but not in relation to volcanic activity. Deciphering
755 the ancient DNA sequence of HM response genes such as *ZmHMA1* in paleobotanical
756 maize specimens found in Central Mexico could help determine if its genetic diversity was
757 already reduced by 5,300 to 6,200 yr BP (Ramos-Madrigal et al., 2016 ; Vallebueno-
758 Estrada et al., 2016; Benz, 2001). Our results open the possibility for environmental
759 changes caused by volcanic activity acting as a driving force in the selection of loci
760 involved in adaptive responses such as heavy metal tolerance.

761

762

763 **Materials and Methods**

764

765 *Plant materials and growth conditions.*

766 Seeds from maize inbred line W22, teosinte *parviglumis* accession CIMMYTMA 29791,
767 and insertional line *LANMu1029790* were sterilized using a 1:1 distilled water and bleach
768 solution, rinsed three times in water, and germinated in MS solid medium. One week-old
769 seedings were transplanted into PVC tubes (length: 90 cm; diameter: 20 cm) or 20-liter
770 pots filled with a pre-sterilized mix composed of 30% peat moss, 10% vermiculite, 10%
771 perlite, and 50% ground litter, complemented with 15-9-12 (N-P-K) Osmocote^{TM} fertilizer.

772 For HM growth conditions, 16 mg/kg of cadmium chloride ($CdCl_2$) and 400 mg/kg of
773 copper sulfate ($CuSO_4$) were added to the substrate before seedling transplant. All plants
774 were grown under glasshouse conditions at 28°C during day and 24°C during night, with
775 relative humidity comprised between 40 and 50%.
776
777
778
779 *Phenotypic analysis.*
780 All plants were harvested at 15 days (V2 stage), 30 days (V6 stage), and 50 days (R1 stage)
781 after transplant. No less than ten plants per biological replicate were measured for each
782 trait and stage, with three biological replicates per experiment. The width and length of
783 immature leaves was measured in the 5th leaf. The length and width of mature leaves in the
784 3rd leaf. The total number of leaves, total number of stem internodes, plant height, basal
785 stem diameter, total number of stem ramifications, and total fresh and dry weight of the
786 aerial biomass were estimated at the R1 stage. Estimated root traits included the number
787 and length of brace roots (aerial roots), the number and length of crown roots (underground
788 roots originating within 2 cm below the basal node), number and length of nodal roots
789 (underground roots originating more than 2 cm below the basal node), the number and
790 length of seminal roots and maximum length of the root system. Statistical analyses were
791 conducted using RStudio, version 4.3.0 (Horton and Kleinman 2015). The data are
792 presented as mean ± standard deviation and were tested by a paired Student's T-Test. When
793 the effects were significant according to T-Test, the treatments were compared with the
794 Welch two sample T-Test at $P < 0.05$.
795
796 *Genetic diversity analysis.*
797 The SNP collection of maize chromosome 5 was analyzed on the basis of the HapMap
798 V3.2.1 dataset (Bukowski et al. 2018), selecting individuals from maize landraces (LR)
799 (Table S6) and teosinte *parviglumis* inbred line accessions (Teo; Table S7). A sliding
800 window diversity (π) was calculated using VCFtools v0.1.13 (Danecek et al. 2011) with a
801 window size of 100 bp (--window-pi 100) and a sliding step of 50 bp (--window-pi-step
802 50). Regions under selection were extracted from a list of 304 genes with domestication-

803 related selection signatures across the whole chromosome (Hufford et al. 2012; Tables S8),
804 for a total of 385,829 sliding windows (Table S9 and S10). A second set of neutral gene
805 regions comprising 2,373,010 windows was also extracted across the entirety of
806 chromosome 5. These two collections were compared to *ZmHMA1* (GRMZM2G067853),
807 *ZmHMA7* (GRMZM2G029951), and *ZmSKUs5* (GRMZM2G076985), encompassing
808 2,743 windows (Table S11 and S12). Additionally, we analyzed genetic diversity in the
809 neighboring regions of these candidate genes, which included six genes
810 (*GRMZM2G701784*, *GRMZM2G014508*, *GRMZM2G367857*, *GRMZM2G375607*,
811 *GRMZM2G374375*, and *GRMZM2G067883*), totaling 3,088 windows. We employed a
812 custom Perl script (Vallebueno GitHub repository) to calculate two diversity metrics: fold
813 change (FC= π(LR)/π(Teo)) and the proportional diversity (FP=π(LR)/(π(LR) + π(Teo)).
814 Data visualization was performed using violin plots generated in R v4.2.2.
815
816 For an arbitrary locus encompassing 30 Kbs up and downstream of the coding sequence of
817 *ZmMA1*, *ZmHMA7*, and *ZmSKUs5*, the number of segregating sites (S), the number of
818 unique sequences (haplotypes, h), and the nucleotide diversity index (θ) were estimated
819 using DnaSP version 6.0 for all accessions included in HapMap3 (Rozas et al. 2017;
820 Bukowski et al. 2018). DnaSP was also used to estimate Tajima's D, Fu and Li's D, and
821 Fu and Li's F indexes (Tajima 1989; Fu and Li 1993). The average proportion of pairwise
822 nucleotide differences per nucleotide site (π) was calculated with VCFtools using bins of
823 100 bp and steps of 25 bp (Tajima 1983; Weir and Cockerham 1984). Null hypothesis of
824 equality of parameters followed two-tailed tests as previously described (Rozas et al.
825 2017).
826
827 To characterize genetic diversity across a 11.47 Mb genomic interval encompassing the
828 ZmHMA1 to *ZmSKUs5* segment on chr.5, we quantified nucleotide diversity (π)
829 differences between maize and teosinte *parviglumis*. For each gene found within the
830 segment, three regions were defined: an upstream region, the coding sequence (CDS), and
831 a downstream region. Nucleotide diversity for each subspecies was calculated within each
832 region and expressed as the ratio πMaize/πTeosinte (πM/πT). Subregions in which maize
833 retained less than 70% of teosinte *parviglumis* diversity (π_M/π_T ≈ 0.7) were highlighted

834 in Supplemental File 6. Genome-wide π estimates were derived from non-overlapping 100
835 bp windows that had been intersected between species. Two complementary statistical
836 approaches were used to evaluate species differences per region. First, a parametric
837 analysis of variance (ANOVA) was fitted for each region using π as the response variable
838 and subspecies (maize vs teosinte *parviglumis*) as a fixed factor. ANOVA was used when
839 its assumptions (approximate normality of residuals and homogeneity of variances) were
840 considered acceptable following Fischer. Second, a paired Wilcoxon signed-rank test was
841 applied to the paired π values from maize and teosinte *parviglumis* within each region as a
842 distribution-free alternative robust to departures from normality and to outliers (Wilcoxon,
843 1945). P-values from both methods were adjusted to control the false discovery rate (FDR)
844 using the Benjamini–Hochberg procedure (Benjamini & Hochberg, 1995). All data
845 processing and statistical analyses were performed in R (version 4.3.1). Gene annotations
846 were obtained from Phytozome using the *Zea mays* PHJ40 v1.2 annotation (Bornowski et
847 al., 2021).
848
849 *Gene expression analysis.*
850 Leaves, stems, tassels, female inflorescences, as well as primary, nodal, and crown roots
851 were manually isolated, frozen in liquid nitrogen and stored at 4°C. Total RNA was
852 extracted using TRIZOL (Thermo Fisher Scientific, USA). For reverse-transcriptase PCR
853 (RT-PCR), RNA was converted to coding DNA using the One-step RT-PCR kit (QIAGEN,
854 USA). The full list of primers is presented in Table S8. *ZmCDK* was used as a positive
855 control. PCR amplification was conducted using the following parameters: at 94°C for 5
856 min.; 94°C 30 sec., 60°C 30 sec., 72°C 1 min. for 35 cycles; final stop after 72°C for 10
857 min. For quantitative real-time PCR (qPCR), total RNA was isolated from 4-week-old
858 meristems using TRIZOL. Complementary DNA (cDNA) was synthesized using 4 µg of
859 total RNA, 10 mM oligodTs and Superscript reverse transcriptase II (Invitrogen, USA).
860 Primers for PCR were designed using the online program Primer 3 Plus (v.0.4.0) and
861 verified with Oligocalculator (Sigma Chemical, St Louis MO) to discard dimer formation.
862 PCR efficiencies of target and reference gene were determined by generating standard
863 curves based on serial dilutions prepared for cDNA templates. PCR efficiency was
864 calculated according to the slope of the standard curve (primers with 100% efficiency, the

865 fold equals 2). Each quantitative real-time PCR (qPCR) reaction was performed in a 10 µl
866 volume consisting of 5 µl of 23 SYBR Green PCR reaction Mix (Applied Biosystems,
867 Foster City, CA). 3.5 µl of the DNA template (100 ng/ml), 0.5 µl of the forward primer (5
868 mM), 0.5 µl of the reverse primer (5 mM), and 0.5 µl of ultrapure water. The qPCR
869 reactions were performed using the CFX96 Touch Real-Time PCR detection System and
870 the data were analyzed using the Bio-Rad CFX Manager software v3.1. The thermal profile
871 consisted of 10 min at 95°C, 40 cycles of 15 sec at 95°C, and 1 min at 60°C. Amplification
872 results were collected at the end of the extension step. Primer sequences for qPCR
873 amplification are listed in Table S7. A comparative 2-ΔΔCT method was used for
874 determining a relative target quantity of gene expression (Schefe et al. 2006), and the
875 cyclin-dependent kinase gene *ZmCDK* (GRMZM2G149286) was used as a control (Hu et
876 al. 2019). Reproducibility of the results was evaluated for each sample by running three
877 technical and three biological replicates of each of the reactions and each sample.
878

879 **Acknowledgments**

880 We would like to thank Ueli Grossniklaus for critical comments of this manuscript; Juana
881 de la Cruz for supporting greenhouse activities; Ivan López-Valdivia, Eduardo González-
882 Orozco and Cristian Eduardo Martínez Guerrero for help with bioinformatic analysis; and
883 Enrique Pola for help with qPCR analysis. All members of the Apolab offered valuable
884 suggestions and support. This research was funded by Conahcyt grant (CB-256826) and
885 the INAH-Cinvestav Tehuacán Collaborative Initiative. J.A-B. is the recipient of a
886 graduate scholarship from Consejo Nacional de Humanidades Ciencia y Tecnologia
887 (CONAHCyT).
888

889 **Competing interests**

890 None declared.
891

892 **Author contributions**

893 J. A-B and J.P.V-C designed the study. J. A-B and J.P.V-C coordinated and managed the
894 project. M.V.E. designed and performed computational analysis. J.A-B performed the

experiments, J. A-B, M.V.E and J.P.V-C generated, analyzed and interpreted data J. A-B and J.P.V-C wrote the article. All authors read and approved the final version of the manuscript.

List of References

AbdElgawad H, Zinta G, Hamed BA, Selim S, Beemster G, Hozzein WN, Wadaan MAM, Asard H, Abuelsoud W. 2020. Maize roots and shoots show distinct profiles of oxidative stress and antioxidant defense under heavy metal toxicity. *Environmental Pollution* 258: 113705.

Acosta-Bayona J, León-Martínez G, Vielle-Calzada JP. 2024. Origin and diversification of maize: two teosintes but different contributions. *Molecular Plant* 17: 233–235.

Aguirre-Liguori JA, Gaut BS, Jaramillo-Correa JP, Tenaillon MI, Montes-Hernández S, García- Oliva F, Hearne SJ, Eguiarte LE. 2019. Divergence with gene flow is driven by local adaptation to temperature and soil phosphorus concentration in teosinte subspecies (*Zea mays parviglumi*s and *Zea mays mexicana*). *Molecular Ecology* 28: 2814–2830.

Arce JL, Macías JL, Vázquez-Selem L. 2003. The 10.5 ka Plinian eruption of Nevado de Toluca, Mexico: stratigraphy and hazard implications. *Geological Society of America Bulletin* 115:230–248

Atta MI, Zehra SS, Ali H, Ali B, Abbas SN, Aimen S, Sarwar S, Ahmad I, Hussain M, Al-Ashkar I, Elango D, Sabagh AE, et al. 2023. Assessing the effect of heavy metals on maize (*Zea mays L.*) growth and soil characteristics: Plants-implications for phytoremediation. *PeerJ* 11: e16067.

925 **Axelsen KB, Palmgren MG. 2001.** Inventory of the superfamily of P-Type ion pumps in
926 *Arabidopsis*. *Plant Physiology* 126: 696-706.
927
928 **Benjamini Y, Hochberg, Y. 1995.** Controlling the false discovery rate: a practical and
929 powerful approach to multiple testing. *Journal of the Royal Statistical Society*, Series
930 B, 57: 289–300.
931
932 **Benke A, Stich B. 2011.** An analysis of selection on candidate genes for regulation,
933 mobilization, uptake, and transport of iron in maize. *Genome* 54: 674–683.
934
935 **Benz BF, Iltis HH. 1992.** Evolution of Female Sexuality in the Maize Ear (*Zea Mays* L. subsp.
936 *Mays-Gramineae*). *Economic Botany* 46: 212–22.
937
938 **Benz B. 2001.** Archaelogical evidence of teosinte domestication from Guilá Naquitz,
939 Oaxaca. *Proceedings of the National Academy of Sciences USA* 98:2104-2106.
940
941 **Bloomfield K, Sánchez-Rubio G, Wilson L. 1977.** Plinian eruptions of Nevado de
942 Toluca Volcano. *Geologische Rundschau* 66:120–146
943
944 **Bomblies K, Doebley JF. 2006.** Pleiotropic effects of the duplicate maize
945 *FLORICAULA/LEAFY* genes *zfl1* and *zfl2* on traits under selection during maize
946 domestication. *Genetics* 172: 519–531.
947
948 **Boutigny S, Sautron E, Finazzi G, Rivasseau C, Frelet-Barrand A, Pilon M, Rolland**
949 **N, Seigneurin-Berny D. 2014.** HMA1 and PAA1, two chloroplast-envelope PIB-
950 ATPases, play distinct roles in chloroplast copper homeostasis. *Journal of*
951 *Experimental Botany* 65: 1529–1540.
952
953 **Bornowski N, Michel KJ, Hamilton JP, Ou, S, Seetharam AS, Jenkins J, Grimwood**
954 **J, Plott C, Shu S, Talag J, Knnedy M, Hundley H, Singan VR, Barry K, Daum C,**
955 **Yoshinaga Y, Schmutz J, Hirsch CN, Hufford MB, de Leon N, Kaeppler SM,**

Buell CR. 2021. Genomic variation within the maize stiff-stalk heterotic germplasm pool. *The Plant Genome*, 14(3): e20114.

Bukowski R, Guo X, Lu Y, Zou C, He B, Rong Z, Wang B, Xu D, Yang B, Xie C, Fan L, Gao S, Xu X, Zhang G, Li Y, Jiao Y, Doebley JF, Ross-Ibarra J, Lorant A, Buffalo V, Cinta Romay M, Buckler ES, Ware D, Lai J, Sun Q, Xu Y. 2018. Construction of the third-generation *Zea mays* haplotype map. *GigaScience* 7: 1-12.

Burton AL, Brown KM, Lynch JP. 2013. Phenotypic diversity of root anatomical and architectural traits in *Zea* species. *Crop Science* 53: 1042–1055.

Cao Y, Zhao X, Liu Y, Wang Y, Wu W, Jiang Y, Liao C, Xu X, Gao S, Shen Y, Lan H, Zou C, Pan G, Lin H, et al. 2019. Genome-wide identification of *ZmHMAs* and association of natural variation in *ZmHMA2* and *ZmHMA3* with leaf cadmium accumulation in maize. *PeerJ* 7: e7877.

Chen Z, Sun J, Li D, Li P, He K, Ali F, Mi G, Chen F, Yuan L, Pan Q, et al. 2022. Plasticity of root anatomy during domestication of a maize-teosinte derived population. *Journal of Experimental Botany* 73: 139–153.

Danecek, Petr, Adam Auton, Goncalo Abecasis, Cornelis A. Albers, Eric Banks, Mark A. DePristo, Robert E. Handsaker, et al. 2011. The Variant Call Format and VCFtools. *Bioinformatics* 27(15): 2156–2158.

Doebley J, Stec A. 1993. Inheritance of the morphological differences between maize and teosinte: comparison of results for two F2 populations. *Genetics* 134: 559-570.

Doebley J, Stec A, Hubbard L. 1997. The evolution of apical dominance in maize. *Nature* 6724: 236-239.

986 **Eyre-Walker A, Gaut RL, Hilton H, Feldman DL, Gaut BS. 1998.** Investigation of the
987 bottleneck leading to the domestication of maize. *PNAS* 95: 4441-4446.
988
989 **Fengxia H, Liang Y, Sang M, Zhao G, Song J, Liu P, Zou C, Chen Z, Ma L, Shen Y.**
990 2025. Complex regulatory network of ZmbZIP54mediated Pb tolerance in maize.
991 *Plant Physiology and Biochemistry* 224: 109945
992
993 **Fu Y-X, Li W-H. 1993.** Statistical tests of neutrality of mutations. *Genetics* 133: 693-709.
994
995 **Gallo-Franco JJ, Sosa CC, Ghneim-Herrera T, Quimbaya M. 2020.** Epigenetic control
996 of plant response to heavy metal stress: a new view on aluminum tolerance. *Frontiers*
997 *in Plant Science* 11: 602625.
998
999 **Gao C, Gao K, Yang H, Ju T, Zhu J, Tang Z, Zhao L, Chen Q. 2022.** Genome-wide
1000 analysis of metallothionein gene family in maize to reveal its role in development and
1001 stress resistance to heavy metal. *Biological Research* 55:1.
1002
1003 **Gao J, Zhang Y, Lu C, Peng H, Luo M, Li G, Shen Y, Haiping D, Zhang Z, Pan G,**
1004 **Lin H.** 2015. The development dynamics of the maize root transcriptome responsive
1005 to heavy metal Pb pollution. *Biochemical and Biophysical Resaearch*
1006 *Communications* 458: 287-293.
1007
1008 **Gaudin ACM, McClymont SA, Raizada MN. 2011.** The nitrogen adaptation strategy of
1009 the wild teosinte ancestor of modern maize, *Zea mays* subsp. *parviglumis*. *Crop*
1010 *Science* 51: 2780–2795.
1011
1012 **Hall JL. 2002.** Cellular mechanisms of heavy metal detoxification and tolerance. *Journal*
1013 *of Experimental Botany* 53: 1-11.
1014
1015 **Hirayama T, Kieber JJ, Hirayama N, Kogan M, Guzman P, Nourizadeh S, Alonso**
1016 **JM, Dailey WP, Dancis A, Ecker JR, et al. 1999.** RESPONSIVE-TO-

1017 ANTAGONIST1, a Menkes/Wilson disease-related copper transporter, is required for
1018 ethylene signaling in *Arabidopsis*. *Cell* 97: 383-393.
1019
1020 **Horton NJ, Kleinman, K. 2015.** Using R and RStudio for data management, statistical
1021 analysis, and graphics second edition. New York, US: Chapman and Hall/CRC.
1022
1023 **Hu B, Jiang Z, Wang W, Qiu Y, Zhang Z, Liu Y, Li A, Gao X, Liu L, Qian Y, Huang**
1024 **X, Yu F, Kang S, Wang Y, Xie J, Cao S, Zhang L, Wang Y, Xie Q, Kopriva S,**
1025 **Chu C, et al. 2019.** Nitrate–NRT1.1B–SPX4 cascade integrates nitrogen and
1026 phosphorus signaling networks in plants. *Nature Plants* 5: 401–413.
1027
1028 **Hufford, Matthew B., Xun Xu, Joost van Heerwaarden, Tanja Pyhäjärvi, Jer-Ming**
1029 **Chia, Reed A. Cartwright, Robert J. Elshire, et al. 2012.** Comparative population
1030 genomics of maize domestication and mprovement. *Nature Genetics* 44 (7): 808–11.
1031
1032 **Larson G, Piperno DR, Allaby RG, Purugganan MD, Andersson L, Arroyo-Kalin M,**
1033 **Barton L, Vigueira CC, Denham T, Dobney K, Doust AN, Gepts P, Thomas M**
1034 **Gilbert P, Gremillion KJ, Lucas L, Lukens L, Marshall FB, Olsen KM, Pires**
1035 **JC, Richerson PJ, Rubio De Casas R, Sanjur OI, Thomas MG, Fuller DQ, et al.**
1036 **2014.** Current perspectives and the future of domestication studies. *PNAS* 111: 6139–
1037 6146.
1038
1039 **Lemmon Zh, Doebley JF. 2014.** Genetic dissection of a genomic region with pleiotropic
1040 effects on domestication traits in maize reveals multiple linked QTL. *Genetics* 198:
1041 345-353
1042
1043 **Lescot M, Déhais P, Thijs G, Marchal K, Moreau Y, Van de Peer Y, Rouzé P,**
1044 **Rombauts S. 2002.** PlantCARE, a database of plant *cis*-acting regulatory elements
1045 and a portal to tools for *in silico* analysis of promoter sequences. *Nucleic Acids*
1046 *Research* 30: 325–327.
1047

Lopez-Valdivia I, Perkins AC, Schneider HM, Vallebueno-Estrada M, Burridge JD, Gonzalez-Orozco E, Montufar A, Montiel R, Lynch JP, Vielle-Calzada JP, et al. 2022. Gradual domestication of root traits in the earliest maize from Tehuacán. *PNAS* 119: e2110245119.

Lorant A, Ross-Ibarra J, Tenaillon M. 2020. Genomics of long- and short-term adaptation in maize and teosintes. *Methods in Molecular Biology* 2090: 289-311.

Lozano-Garcia S, Torres-Rodriguez E, Ortega B, Vázquez G, Caballero M. 2013. Ecosystem responses to climate disturbances in western central Mexico during the late Pleistocene and Holocene. *Palaeography, Palaecoclimatology, Palaecology* 370: 184-195

Ludlow-Wiechers B, Almeida-Leñero L, Isble G. 2005. Paleoecological and climatic changes of the Upper Lerma Basin, Central Mexico during the Holocene. *Quaternary Research* 64: 318-332.

Macías JL, García-Palomo A, Arce JL, Siebe C, Espíndola JM, Komorowski JC, Scott K. 1997. *Late Pleistocene-Holocene cataclysmic eruptions at Nevado de Toluca and Jocotitlan volca- noes, central Mexico. In Proterozoic to recent stratigraphy, tectonics, and volcanology: Utah, Nevada, southern Idaho, and central Mexico* (Link PK, Kowallis BJ Eds,) Geology Studies, 42. Brigham Young University, Provo, pgs 493–528.

Macías JL. 2005. Geología e historia eruptiva de algunos de los grandes volcanes activos de México. *Boletín De La Sociedad Geológica Mexicana*. 107: 379-424.

Macías JL, Arce JL. 2019. Volcanic activity in Mexico during the Holocene. In *The Holocene and Anthropocene Environmental History of Mexico* (Torrescano-Valle N. Islebe GA, and Priyadarsi DR Eds), Springer Nature Switzerland; pgs 129-170.

1079 **Malenica N, Dunić JA, Vukadinović L, Cesar V, Šimić D. 2021.** Genetic approaches to
1080 enhance multiple stress tolerance in maize. *Genes* 12:1760.
1081
1082 **Martín-Trillo M, Cubas P. 2010.** TCP genes: a family snapshot ten years later. *Trends in*
1083 *Plant Science* 15: 31–39.
1084
1085 **Matsuoka Y, Vigouroux Y, Goodman MM, Sanchez JG, Buckler E, Doebley J. 2002.**
1086 A single domestication for maize shown by multilocus microsatellite genotyping.
1087 *PNAS* 99: 6080-6084.
1088
1089 **McCarty DR, Mark Settles A, Suzuki M, Tan BC, Latshaw S, Porch T, Robin K,**
1090 **Baier J, Avigne W, Lai J, Messing J, Koch KE, Curtis Hannah L, et al. 2005.**
1091 Steady-state transposon mutagenesis in inbred maize. *Plant Journal* 44: 52–61.
1092
1093 **Mikkelsen MD, Pedas P, Schiller M, Vincze E, Mills RF, Borg S, Møller A,**
1094 **Schjoerring JK, Williams LE, Baekgaard L, Holm PB, Palmgren MG, et al. 2012.**
1095 Barley *HvHMA1* is a heavy metal pump involved in mobilizing organellar Zn and Cu
1096 and plays a role in metal loading into grains. *PLoS ONE* 7: e49027.
1097
1098 **Perkins AC, Lynch JP. 2021.** Increased seminal root number associated with
1099 domestication improves nitrogen and phosphorus acquisition in maize seedlings.
1100 *Annals of Botany* 128: 453–468.
1101
1102 **Pickersgill B. 2007.** Domestication of plants in the Americas: insights from mendelian and
1103 molecular genetics. *Annals of Botany* 100: 925–940.
1104
1105 **Piperno DR, Moreno JE, Iriarte J, Holst I, Lachniet M, Jones JG, Ranere J, Castanzo**
1106 **R. 2007.** Late Pleistocene and Holocene environmental history of the Iguala Valley,
1107 Central Balsas Watershed of Mexico. *Proceedings of the National Academy of*
1108 *Sciences USA* 104: 11874-11881
1109

1110 **Piperno DR, Holst I, Winter K, McMillan O. 2015.** Teosinte before domestication:
1111 experimental study of growth and phenotypic variability in late Pleistocene and early
1112 Holocene environments. *Quaternary International* 363: 65–77.
1113
1114 **Ramos-Madrigal J, Smith BD, Moreno-Mayar J, Gopalakrishnan S, Ross-Ibarra J,**
1115 **Gilbert MTP, Wales N. 2016.** Genome sequence of a 5,310-year-old maize cob
1116 provides insights into the early stages of maize domestication. *Current Biology*
1117 26:3195-3201
1118
1119 **Ren W, Zhao L, Liang J, Wang L, Chen L, Li P, Liu Z, Li X, Zhang Z, Li J, He K,**
1120 **Zhao Z, Ali F, Mi G, Yan J, Zhang F, Chen F, Yuan L, Pan Q, et al. 2022.** Genome-
1121 wide dissection of changes in maize root system architecture during modern breeding.
1122 *Nature Plants* 8: 1408–1422.
1123
1124 **Ross-Ibarra J, Morrell PL, Gaut BS. 2007.** Plant domestication, a unique opportunity to
1125 identify the genetic basis of adaptation. *PNAS* 104: 8641-8648.
1126
1127 **Rozas J, Ferrer-Mata A, Sanchez-Del Barrio JC, Guirao-Rico S, Librado P, Ramos-**
1128 **Onsins SE, Sanchez-Gracia A. 2017.** DnaSP 6: DNA sequence polymorphism
1129 analysis of large data sets. *Molecular Biology and Evolution* 34: 3299–3302.
1130
1131 **Schefe JH, Lehmann KE, Buschmann IR, Unger T, Funke-Kaiser H. 2006.**
1132 Quantitative real-time RT-PCR data analysis: current concepts and the novel "gene
1133 expression's CT difference" formula. *Journal of Molecular Medicine* 84: 901–910.
1134
1135 **Sedbrook JC, Carroll KL, Hung KF, Masson PH, Somerville CR. 2002.** The
1136 *Arabidopsis SKU5* gene encodes an extracellular glycosyl phosphatidylinositol-
1137 anchored glycoprotein involved in directional root growth. *Plant Cell* 14: 1635–1648.
1138

1139 **Shen Y, Zhang Y, Chen J, Haijian L, Zhao M, Peng H, Liu L, Yuan G, Zhang S,**
1140 **Zhang Z, Pan G.** 2013. Genome expression profile analysis reveals important
1141 transcripts in maize roots responding to the stress of heavy metal Pb. *Physiologia*
1142 *Plantarum* 147:270-82.
1143
1144 **Siebe C, Macías JL, Abrams M, Rodríguez S, Castro R. 1997.** Catastrophic prehistoric
1145 eruptions at Popocatépetl and Quaternary explosive volcanism in the Serdán-oriental
1146 basin, East-central México. *IAVCEI General Assembly*, 88 pg.s
1147
1148 **Siebe C, Macías JL. 2006.** Volcanic hazards in the Mexico City metropolitan area from
1149 eruptions at Popocatépetl, Nevado de Toluca, and Jocotitlán stratovolcanoes and
1150 monogenetic sco- ria cones in the Sierra Chichinautzin volcanic field. In *Neogene-*
1151 *Quaternary continental margin volcanism: a perspective from Mexico* (Siebe C,
1152 Macías JL, Aguirre G Eds.) *Geological Society of America Special Paper* 402: 253–
1153 329.
1154
1155 **Sigmon B, Vollbrecht E. 2010.** Evidence of selection at the *ramosa1* locus during maize
1156 domestication. *Molecular Ecology* 19: 1296–1311.
1157
1158 **Smeets K, Opdenakker K, Remans T, Van Sanden S, Van Belleghem F, Semane B,**
1159 **Horemans N, Guisez Y, Vangronsveld J, Cuypers A, et al. 2009.** Oxidative stress-
1160 related responses at transcriptional and enzymatic levels after exposure to Cd or Cu in
1161 a multipollution context. *Journal of Plant Physiology* 166: 1982–1992.
1162
1163 **Solioz M, Vulpe C. 1996.** CPx-type ATPases: a class of P-type ATPases that pump heavy
1164 metals. *Trends in Biochemical Sciences* 21: 237-241.
1165
1166 **Studer AJ, Wang H, Doebley JF. 2017.** Selection during maize domestication targeted a
1167 gene network controlling plant and inflorescence architecture. *Genetics* 207: 755–765.
1168
1169 **Tajima F. 1983.** Evolutionary relationship of DNA sequences in finite populations.
1170 *Genetics* 105: 437-460.

1171

1172 **Tajima F. 1989.** Statistical method for testing the neutral mutation hypothesis by DNA
1173 polymorphism. *Genetics* 123: 585-595.
1174

1175 **Torrescano-Valle N. Islebe GA, and Priyadarsi DR. 2019.** *The Holocene and*
1176 *Anthropocene Environmental History of Mexico*. Springer Nature Switzerland. 280
1177 pgs
1178

1179 **Vallebueno-Estrada M, Rodriguez-Arevalo I, Rougon-Cardoso A, Martinez**
1180 **Gonzalez J, Garcia Cook A, Montiel R, Vielle-Calzada JP. 2016.** The earliest
1181 maize from San Marcos Tehuacán is a partial domesticate with genomic evidence of
1182 inbreeding. *Proceedings of the National Academy of Sciences USA* 113:14151-14156.
1183

1184 **Vallebueno-Estrada M, Hernández-Robles G, González-Orozco E, López-Valdivia I,**
1185 **Rosales-Tham T, Vásquez-Sánchez V, Swarts K, Dillehay T, Vielle-Calzada JP,**
1186 **Montiel R. 2023**. Domestication and lowland adaptation of coastal preceramic maize
1187 from Paredones, Peru. *Elife* 12: e83149.
1188

1189 **Vielle-Calzada JP, De La Vega OM, Hernández-Guzmán G, Ibarra-LacLette E,**
1190 **Alvarez-Mejía C, Vega-Arreguín JC, Jiménez-Moraila B, Fernández-Cortés A,**
1191 **Corona-Armenta G, Herrera-Estrella L, Herrera-Estrella A. 2009.** The Palomero
1192 genome suggests metal effects on domestication. *Science* 326: 1078.
1193

1194 **Voskoboinik I, Fernando R, Veldhuis N, Hannan KM, Marmy-Conus N, Pearson RB,**
1195 **Camakaris J. 2003.** Protein kinase-dependent phosphorylation of the Menkes copper
1196 P-type ATPase. *Biochemical and Biophysical Research Communications* 303: 337–
1197 342.
1198

1199 **Wang H, Studer AJ, Zhao Q, Meeley R, Doebley JF. 2015.** Evidence that the origin of
1200 naked kernels during maize domestication was caused by a single amino acid
1201 substitution in *tga1*. *Genetics* 200: 965–974.

1202

1203 **Weir BS, Cockerham CC. 1984.** Estimating F-Statistics for the analysis of population
1204 structure. *Evolution* 38: 1358-1370.

1205

1206 **Wilcoxon F**. **1945.** Individual comparisons by ranking methods. *Biometrics Bulletin* 1: 80–
1207 83.

1208

1209 **Williams LE, Mills RF. 2005.** P1B-ATPases - an ancient family of transition metal pumps
1210 with diverse functions in plants. *Trends in Plant Science* 10: 491–502.

1211

1212 **Wills DM, Whipple CJ, Takuno S, Kursel LE, Shannon LM, Ross-Ibarra J, Doebley**
1213 **JF. 2013.** From many, one: genetic control of prolificacy during maize domestication.
1214 *PLoS Genetics* 9: e1003604.

1215

1216 **Yamasaki M, Tenaillon MI, Bi IV, Schroeder SG, Sanchez-Villeda H, Doebley JF,**
1217 **Gaut BS, McMullen MD. 2005.** A large-scale screen for artificial selection in maize
1218 identifies candidate agronomic loci for domestication and crop improvement. *The*
1219 *Plant Cell* 17: 2859-2872

1220 .

1221 **Yang N, Wang Y, Liu X, Jin M, Vallebueno-Estrada M, Calfee E, Chen L, Dilkes BP,**
1222 **Gui S, Fan X, Harper TK, Kennett DJ, Li W, Lu Y, Ding J, Chen Z, Luo J,**
1223 **Mambakkam S, Menon M, Snodgrass S, Veller C, Wu S, Wu S, Zhuo L, Xiao Y,**
1224 **Yang X, Stitzer MC, Runcie D, Yan J, Ross-Ibarra J, et al. 2023.** Two teosintes
1225 made modern maize. *Science* 382: 1013–1021.

1226

1227 **Yang X, Ten J, Lin X, Yang Z, Deng X, He Q.** 2023. Melatonin Alleviates Chromium
1228 Toxicity in Maize by Modulation of Cell Wall Polysaccharides Biosynthesis,
1229 Glutathione Metabolism, and Antioxidant Capacity. *International Journal of*
1230 *Molecular Sciences* 24: 3816.

1231

1232 **Zhang M, Zhao L, Yun Z, Wu X, Wu Q**. **2024.** Comparative transcriptome analysis of
1233 maize (*Zea mays* L.) seedlings in response to copper stress. *Open Life Sciences* 19:
1234 20220953.
1235
1236 **Zhang X, Li M, Ma X, Jin X, Wu X, Zhang H, Guan H, Fu Z, Chen Z, Wang. 2024.**
1237 Transcriptomics Combined with Physiology and Metabolomics Reveals the
1238 Mechanism of Tolerance to Lead Toxicity in Maize Seedling. *Physiologia Plantarum*
1239 176: 14547
1240
1241 **Zhiguo E, Tingting L, Chen C, Lei W. 2018.** Genome-wide survey and expression
1242 analysis of P1B-ATPases in rice, maize and sorghum. *Rice Science* 25: 208–217.
1243

Legend of Figures.

Figure 1. Phenotypic response of teosinte *parviglumis* and wild-type W22 maize grown under heavy metal stress. (**a**) to (**e**), teosinte *parviglumis*; (**f**) to (**j**), W22 maize. (**a**) Teosinte *parviglumis* in absence of heavy metal stress at early flowering stage. (**b**) Teosinte *parviglumis* grown under heavy metal stress at early flowering stage. (**c**) Teosinte *parviglumis* in absence of heavy metal stress at late flowering stage. (**d**) Teosinte *parviglumis* grown under heavy metal stress at late flowering stage. (**e**) Teosinte *parviglumis* showing absence of lateral branching, and proliferation of female inflorescences arising from independent axillary meristems under heavy metal stress (detail of d). (**f**) W22 maize in absence of heavy metal stress at early flowering stage. (**g**) W22 maize grown under heavy metal stress at early flowering stage. (**h**) W22 maize in absence of heavy metal stress at late flowering stage. (**i**) W22 maize grown under heavy metal stress at late flowering stage. (**j**) W22 maize female inflorescences at late flowering stage (detail of i). Scale bars: 10 cm.

Figure 2. Genetic diversity of loci encompassing *ZmHMA1, ZmHMA7*, and *ZmSKUs5.* The nucleotide variability index (π) was calculated for all HapMap3 accessions of teosinte *parviglumis* (blue line), maize (red line), and *Tripsacum dactyloides* (orange line), taking in consideration the coding sequence (arrow) and an upstream and downstream region of 15 Kb encompassing each gene. (**a**) Nucleotide variability in the *ZmHMA1* locus. (**b**) Nucleotide variability in the ZmHMA7 locus. (**c**) Nucleotide variability in the *ZmSKUs5* locus. (**d**) Nucleotide variability in the *ZmGLB1* locus.

1244

1245 **Figure 3. Structure and gene expression of *ZmHMA1* and *ZmHMA7* in teosinte**
1246 ***parviglumis* and W22 maize.** (**a**) Structural analysis of *ZmHMA1*, *ZmHMA7*, and
1247 *ZMSKUs5*. Blue triangles indicate the location of motifs predicted in the regulatory region
1248 of each gene. The insertion site of *Mu* line *LANMu1029790* is indicated by a red triangle.
1249 (**b**) RT-PCR analysis of *ZmHMA1* and *ZMHMA7* expression throughout development of
1250 teosinte *parviglumis* and W22 maize in presence or absence of heavy metal stress; L=leaf;
1251 S=stem; PR=primary root; NR=nodal root; CR=crown root. V2: 15 days after transplant;

1252 V6: 30 days after transplant; R1: 50 days after transplant. Controls: (-) absence of DNA;
1253 (+) genomic DNA. (**c**) qPCR analysis of *ZmHMA1* expression in 1-month old primary
1254 roots, in absence or presence of heavy metal stress. (**d**) qPCR analysis of *ZmHMA7*
1255 expression in 1-month old primary roots, in absence or presence of heavy metal stress.
1256 Histograms in (**c**) and (**d**) show the relative fold-change (normalized to actin, based on
1257 technical and biological triplicates); standard deviations are shown by vertical lines and
1258 Student T-test P-values represented by asterisks. * P<0.01; ** P<0.001.

Figure 4. *Tb1* and *ZmHMA1* expression in the shoot apical meristem of plantlets grown under heavy metal stress. (a) qPCR analysis of *Tb1* expression in 1-month old teosinte *parviglumis* plantlets grown in absence or presence of heavy metal stress. (**b**) qPCR analysis of *ZmHMA1* expression in 1-month old teosinte *parviglumis* and W22 maize plantlets in absence or presence of heavy metal stress. Histograms show the relative fold-change (normalized to actin, based on technical and biological triplicates); standard deviations are shown by vertical lines and Student T-test P-values represented by asterisks; * P<0.01.

1259 **Figure 5. Location and age of volcanic eruptions occurred during the Holocene in**
1260 **comparison to collection sites of teosinte *parviglumis* populations most closely related**
1261 **to maize.** (**a**) Black asterisks correspond to the location and accession numbers of collected
1262 teosinte *parviglumis* populations that are phylogenetically most closely allied with extant
1263 maize, following Matzuoka et al. 2002. The location of 21 volcanoes belonging to the
1264 Michoacan-Guanajuato Volcanic Field is indicated with yellow circles. The locations of
1265 the Nevado de Toluca and Popocatéptl craters are indicated with a red and brown circle,
1266 respectively. Orange squares indicate the location of paleoenvironmental studies covering
1267 from 14,000 cal yr BP to current era, as described in Lozano-García et al. 2013 (i), Piperno
1268 et al. 2007 (ii), and Ludlow-Wiechers et al. 2005 (iii). (**b**) Time versus age of volcanic
1269 eruptions occurred in the map area of the Transmexican Volcanic Belt during the Holocene;
1270 numbers correspond to volcanoes illustrated in (**a**). Adapted from Macías and Arce (2019).

Legend of Appendix and Supplementary Files.

Figure S1. Cumulative plot of QTL detected in a region of chromosome five that includes *ZmSKUs5* and *ZmHMA1* (modified from Lemmon and Doebley, 2014).

Figure S2. Comparison of chromosome 5 nucleotide variability between maize landraces and teosinte *parviglumis*.

Figure S3. Large scale transcriptional comparison of HM response genes across six maize experiments based on fold change >1 and false discovery rate (FDR) < 0.05.

Figure S4. Expression of *ZmHMA1* in wild-type and homozygous *zmhma1* maize individuals.

Figure S5. Distribution of soils of volcanic origin (andosols; pink) in geographic regions of teosinte *parviglumis* populations most closely related to extant maize.

Figure S6. Speculative model illustrating the influence of heavy metal stress on the evolutionary transition of teosinte *parviglumis* to maize.

Table S1. Additional estimation of phenotypic traits in teosinte *parviglumis* grown in absence or presence of heavy metal stress.

Table S2. Additional estimation of phenotypic traits in wild-type and *zmhma1* maize grown in absence or presence of heavy metal stress.

Table S3. Full comparison of phenotypic values for wild-type W22, *zmhma1*, and teosinte *parviglumis* individuals grown under absence or presence of heavy metal stress

Table S4. Nucleotide variability across the *ZmSKUS5, ZmHMA*1 and *ZmHMA7* locus; and their upstream and downstream neighboring genes in maize landraces, maize improved lines, and teosinte *parviglumi*s accessions included in HapMap3.

Table S5. Description of six transcriptomes reporting HM response genes under different growing conditions and developmental stages.

Table S6. Collection of primers used in this study.

Table S7. Maize landrace accessions used in the genetic diversity analysis chr.5.

Table S8. Teosinte *parviglumis* accessions used in the genetic diversity analysis chr.5.

Supplementary File 1. List of domestication genes present on chr5 as defined by Hufford et al. 2012

Supplementary File 2. FC and FP values for all domestication genes present in chr.5.

Supplementary File 3. FC and FP values of neutral regions included in chr.5.

Supplementary File 4. FC and FP values of candidate genes *ZmHMA1*, *ZmHMA7* and *ZmSKUs5.*

Supplementary File 5. FC and FP values of *ZmHMA1*, *ZmHMA7* and *ZmSKUs5* neighboring genes

Supplementary File 6. Genetic diversity in loci across 11.47 Mb of chr.5 in the *ZmSKUs5* to *ZmHMA1* segment

Supplementary File 7. Genetic diversity in loci encompassing heavy metal response genes shared by six transcriptomes with fold change strictly higher than 1 and FDR<0.05

Figure 1

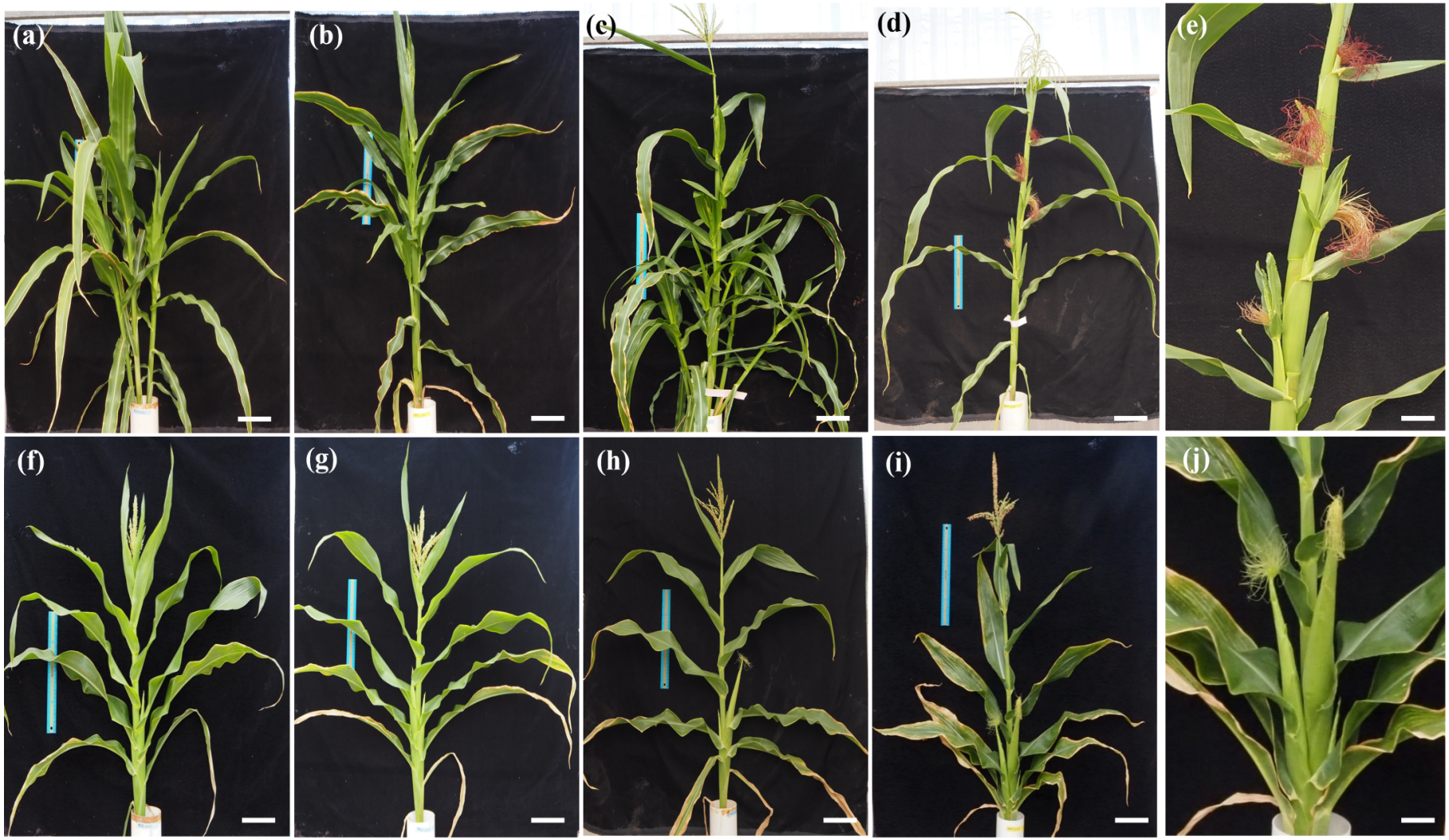

Figure 2.

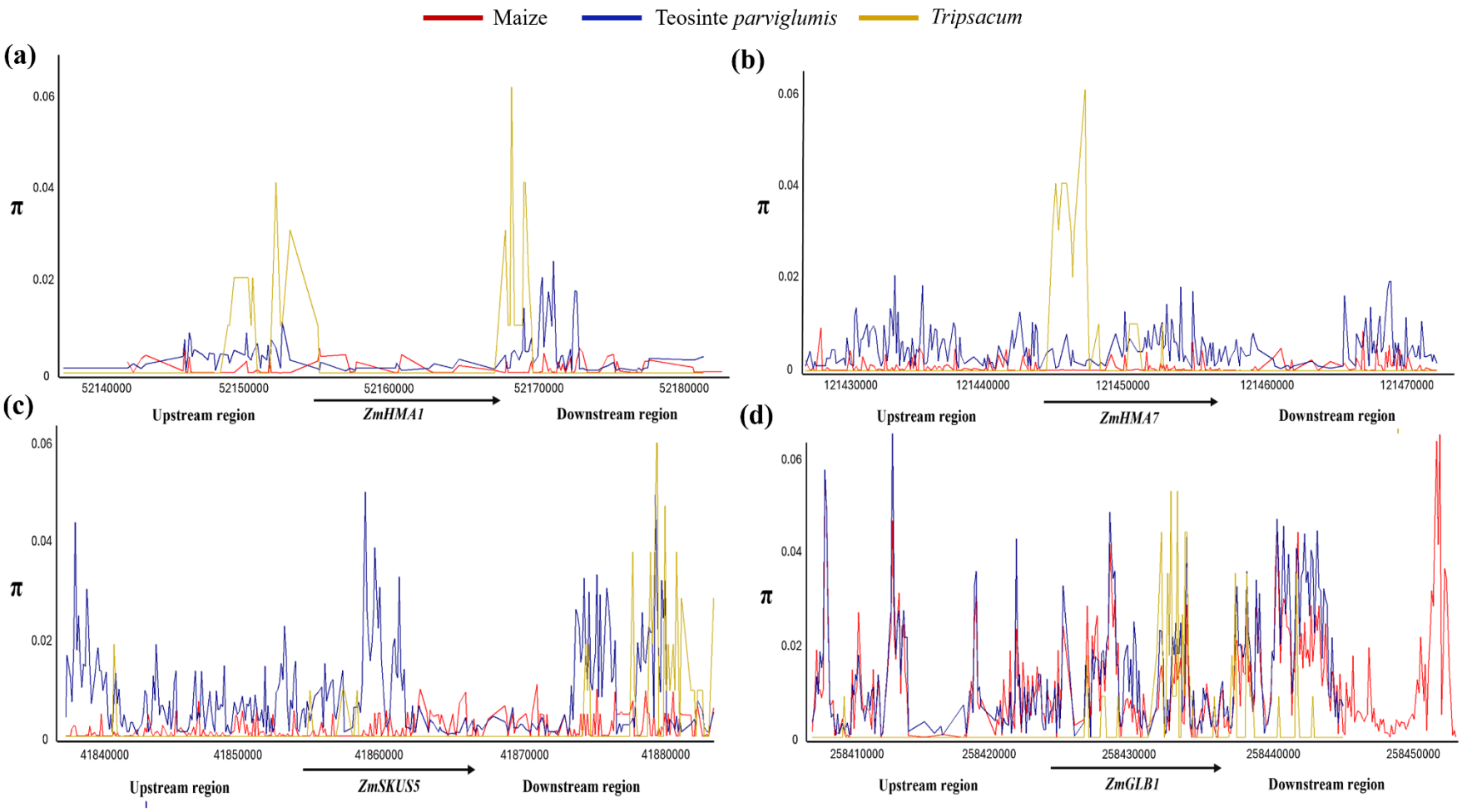
Maize
Teosinte parviglumis
Tripsacum
(a)
(b)
(c)
(d)
π
0.06
0.04
0.02
0
52140000
52150000
52160000
52170000
52180000
121430000
121440000
121450000
121460000
121470000
41840000
41850000
41860000
41870000
41880000
258410000
258420000
258430000
258440000
258450000
Upstream region
ZmHMA1
Downstream region
ZmHMA7
ZmSKUS5
ZmGLB1

Figure 3.

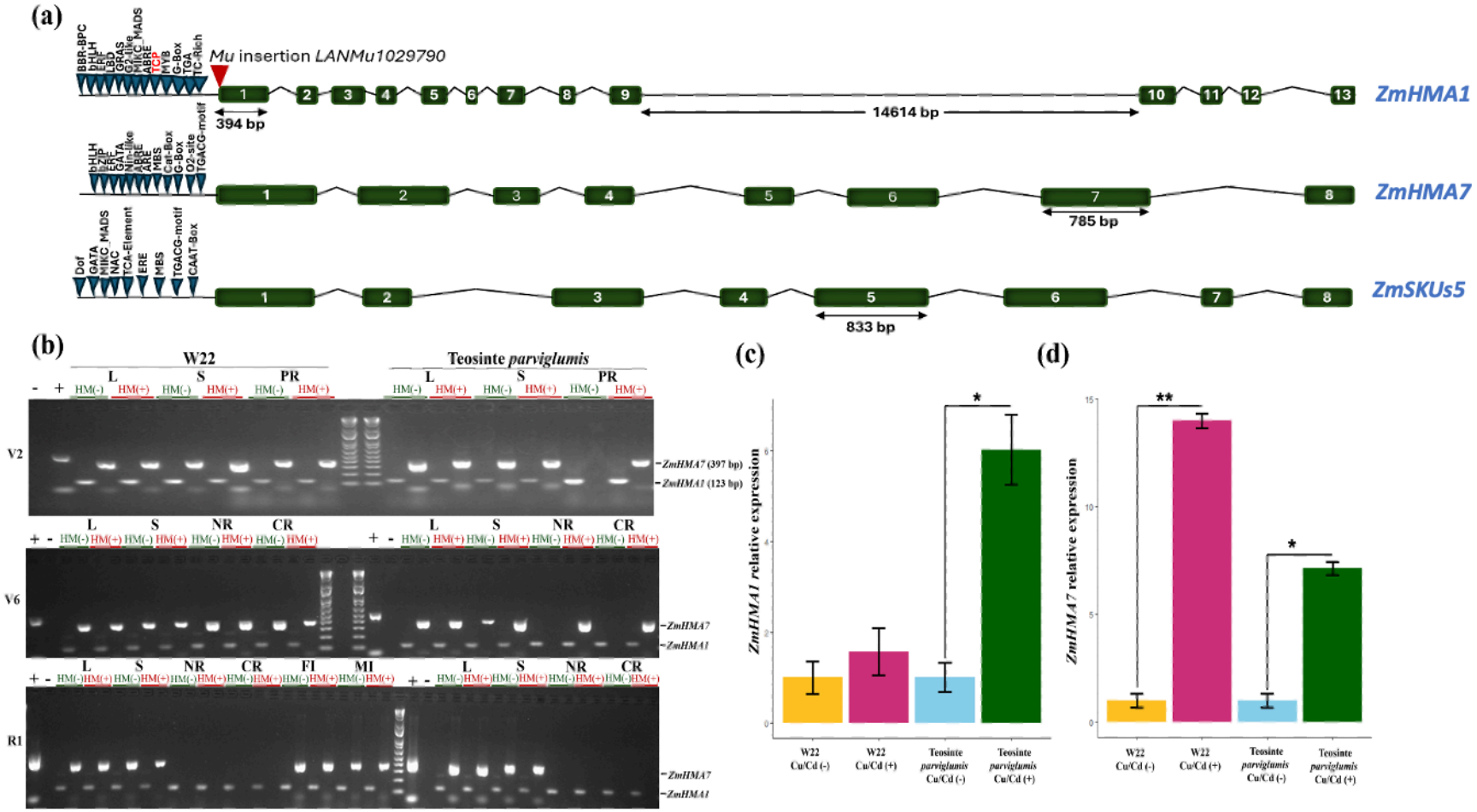
(a)
Mu insertion LANMu1029790
394 bp
14614 bp
ZmHMA1
ZmHMA7
785 bp
ZmSKUs5
833 bp
(b)
W22
Teosinte parviglumis
V2
V6
R1
ZmHMA7 (397 bp)
ZmHMA1 (123 bp)
(c)
ZmHMA1 relative expression
(d)
ZmHMA7 relative expression
W22 Cu/Cd (-)
W22 Cu/Cd (+)
Teosinte parviglumis Cu/Cd (-)
Teosinte parviglumis Cu/Cd (+)

Figure 4.

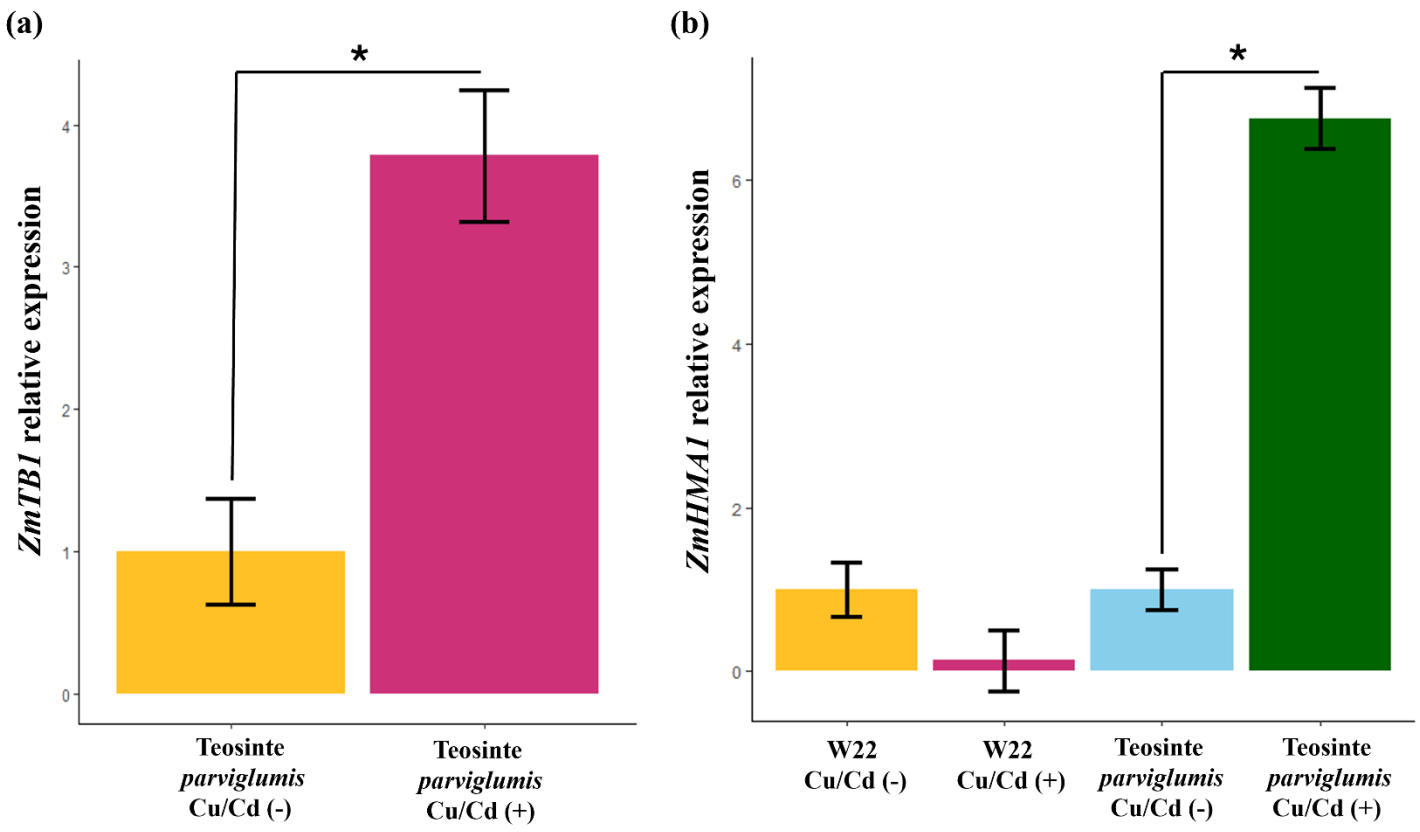
(a)
*
ZmTB1 relative expression
0
1
2
3
4
Teosinte parviglumis Cu/Cd (-)
Teosinte parviglumis Cu/Cd (+)
(b)
*
ZmHMA1 relative expression
0
2
4
6
W22 Cu/Cd (-)
W22 Cu/Cd (+)
Teosinte parviglumis Cu/Cd (-)
Teosinte parviglumis Cu/Cd (+)

Figure 5.

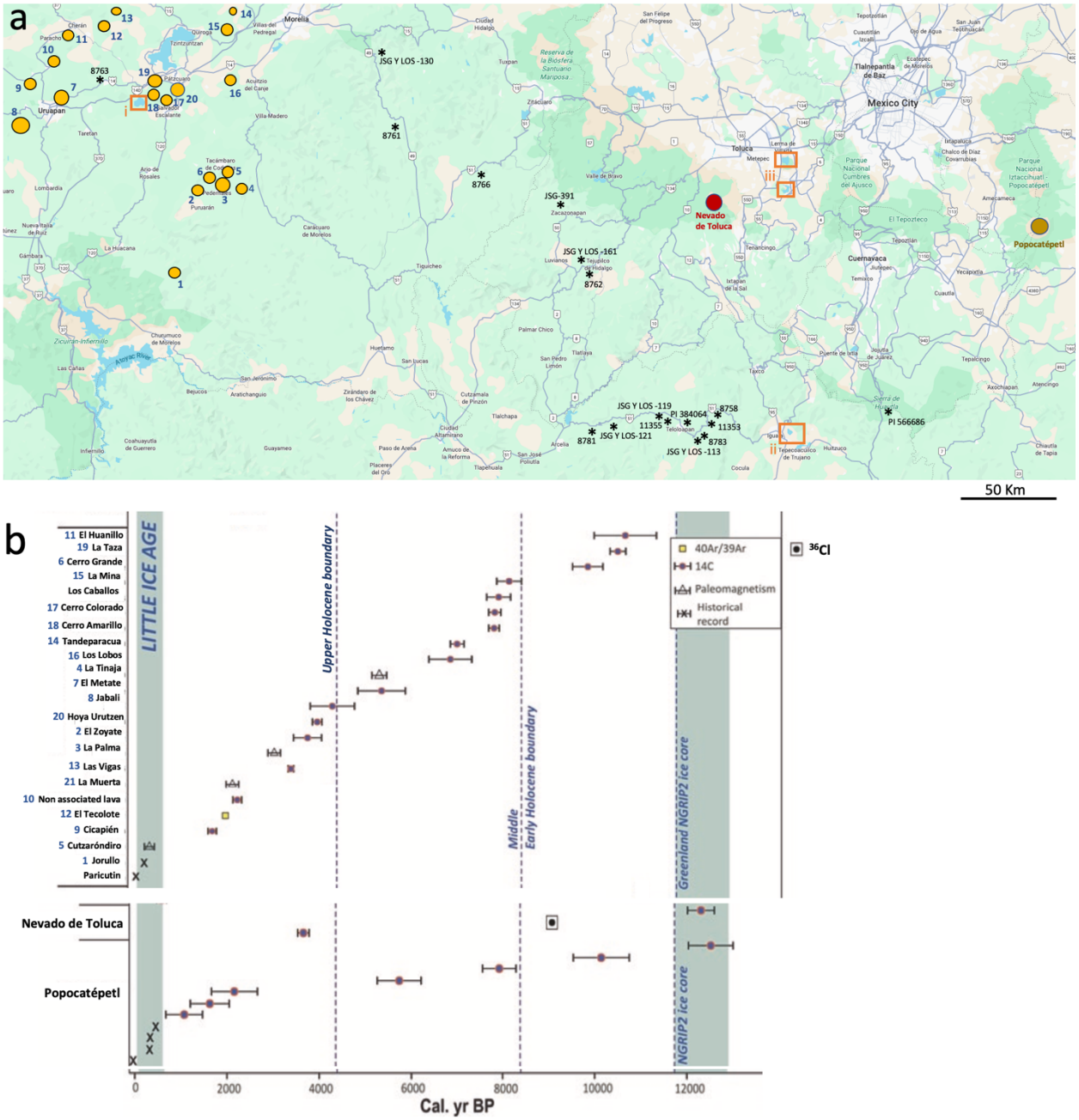
a
Nevado de Toluca
Popocatépetl
Mexico City
Toluca
Cuernavaca
Morelia
Uruapan
JSG Y LOS -130
8761
8766
JSG-391
JSG Y LOS -161
8762
JSG Y LOS -119
PI 384064
8758
11355
11353
8781
JSG Y LOS-121
8783
JSG Y LOS -113
PI 566686
8763
50 Km
b
11 El Huanillo
19 La Taza
6 Cerro Grande
15 La Mina
Los Caballos
17 Cerro Colorado
18 Cerro Amarillo
14 Tandeparacua
16 Los Lobos
4 La Tinaja
7 El Metate
8 Jabali
20 Hoya Urutzen
2 El Zoyate
3 La Palma
13 Las Vigas
21 La Muerta
10 Non associated lava
12 El Tecolote
9 Cicapién
5 Cutzaróndiro
1 Jorullo
Paricutin
LITTLE ICE AGE
Upper Holocene boundary
Middle
Early Holocene boundary
Greenland NGRIP2 ice core
40Ar/39Ar
14C
Paleomagnetism
Historical record
36Cl
Nevado de Toluca
Popocatépetl
NGRIP2 ice core
0
2000
4000
6000
8000
10000
12000
Cal. yr BP

Table 1. Estimation of phenotypic traits in wild-type and *zmhma1* maize grown in absence and presence of heavy metal stress.

			W22			*zmhma1*			W22	*zmhma1*		W22	*zmhma1*	
			Cu/Cd (-)	Cu/Cd (+)		Cu/Cd (-)	Cu/Cd (+)		Cu/Cd (-)	Cu/Cd (-)		Cu/Cd (+)	Cu/Cd (+)	
		Description	**Mean ± SD**	**Mean ± SD**	**P value**	**Mean ± SD**	**Mean ± SD**	**P value**	**Mean ± SD**	**Mean ± SD**	**P value**	**Mean ± SD**	**Mean ± SD**	**P value**
Aerial traits	NL	Number of Leaves	13.40 ± 0.84	12.00 ± 1.70	1.20E-02*	11.40 ± 0.84	11.10 ± 0.74	4.70E-01	13.40 ± 0.84	11.40 ± 0.84	5.00E-05***	12.00 ± 1.70	11.10 ± 0.74	1.42E-01
	LML	Length of Mature Leaf (cm)	77.40 ± 6.64	72.35 ± 8.81	1.54E-01	69.85 ± 9.18	63.85 ± 7.31	1.32E-01	77.40 ± 6.64	69.85 ± 9.18	4.93E-02*	72.35 ± 8.81	63.85 ± 7.31	3.05E-02*
	WML	Width of Mature Leaf (cm)	6.75 ± 1.30	7.20 ± 1.42	4.37E-01	9.75 ± 1.40	9.95 ± 0.86	6.42E-01	6.75 ± 1.30	9.75 ± 1.40	1.00E-04***	7.20 ± 1.42	9.95 ± 0.86	6.00E-05***
	LIL	Length of Immature Leaf (cm)	59.50 ± 6.10	51.90 ± 9.97	5.90E-02	48.25 ± 6.88	45.35 ± 9.43	4.56E-01	59.50 ± 6.10	48.25 ± 6.88	1.12E-03**	51.90 ± 9.97	45.35 ± 9.43	1.49E-01
	WIL	Width of Immature Leaf (cm)	7.45 ± 0.80	6.60 ± 1.10	6.70E-02	9.25 ± 0.72	8.85 ± 0.85	2.78E-01	7.45 ± 0.80	9.25 ± 0.72	5.00E-05***	6.60 ± 1.10	8.85 ± 0.85	7.00E-05***
	HEI	Height (cm)	99.60 ± 32.61	82.20 ± 34.94	3.30E-01	103.15 ± 10.76	125.90 ± 18.81	2.00E-03**	99.60 ± 32.61	103.15 ± 10.76	7.48E-01	82.20 ± 34.94	125.9 ± 18.81	2.66E-03**
	SD	Stem Diameter (cm)	3.24 ± 0.52	2.60 ± 0.53	1.70E-02*	3.02 ± 0.51	2.86 ± 0.59	5.19E-01	3.24 ± 0.52	3.02 ± 0.51	3.49E-01	2.60 ± 0.53	2.86 ± 0.59	3.12E-01
	DWAP	Dry Weight of Aerial Part (g)	28.43 ± 8.04	25.22 ± 8.26	4.38E-01	28.46 ± 9.54	31.44 ± 18.85	6.15E-01	28.43 ± 8.04	28.46 ± 9.54	2.04E-02*	25.22 ± 8.26	31.44 ± 18.85	1.56E-03**
	NSB	Number of Spike Branches	9.00 ± 1.63	7.20 ± 3.16	1.21E-01	13.40 ± 2.32	13.60 ± 1.96	7.87E-01	9.00 ± 1.63	13.40 ± 2.32	1.10E-04***	7.20 ± 3.16	13.60 ± 1.96	4.00E-05***
	NFI	Number of Female Inflorescences	1.20 ± 0.42	0.70 ± 0.67	9.70E-02	1.90 ± 0.32	1.60 ± 0.52	1.42E-01	1.20 ± 0.42	1.90 ± 0.32	5.40E-04***	0.70 ± 0.67	1.60 ± 0.52	3.57E-03***
	WFI	Weight of Female Inflorescences (g)	40.06 ± 14.39	37.75 ± 18.83	7.43E-01	69.53 ± 11.20	76.06 ± 25.04	4.56E−02	40.06 ± 14.39	69.53 ± 11.20	7.00E-05***	37.75 ± 18.83	76.06 ± 25.04	1.13E-03**
Roots traits	NBR	Number of Brace Roots	12.90 ± 4.33	16.30 ± 4.99	1.60E-01	10.60 ± 6.29	9.50 ± 6.79	6.82E-01	12.90 ± 4.33	10.60 ± 6.29	3.54E-01	16.30 ± 4.99	9.50 ± 6.79	2.00E-02*
	LBR	Length of Brace Roots (cm)	16.15 ± 9.75	4.00 ± 2.04	1.00E-03***	15.75 ± 14.03	2.67 ± 2.01	4.00E-03**	16.15 ± 9.75	15.75 ± 14.03	9.42E-01	4.00 ± 2.04	2.67 ± 2.01	1.59E-01
	NCR	Number of Crown Roots	11.30 ± 2.11	7.60 ± 0.97	1.00E-03***	12.10 ± 2.42	9.00 ± 2.58	1.00E-02**	11.30 ± 2.11	12.10 ± 2.42	4.42E-01	7.60 ± 0.97	9.00 ± 2.58	1.26E-01
	LCR	Length of Crown Roots (cm)	58.90 ± 21.87	48.85 ± 11.80	2.02E-01	50.50 ± 1344	44.40 ± 20.75	3.92E-01	58.90 ± 21.87	50.50 ± 1344	3.14E-01	48.85 ± 11.80	44.40 ± 20.75	5.63E-01
	NNR	Number of Nodal Roots	10.50 ± 2.27	6.70 ± 2.79	4.00E-03**	8.50 ± 2.42	8.00 ± 1.56	6.03E-01	10.50 ± 2.27	8.50 ± 2.42	7.26E-02	6.70 ± 2.79	8.00 ± 1.56	2.15E-01
	LNR	Length of Nodal Roots (cm)	87.20 ± 16.80	55.30 ± 21.10	1.00E-03***	50.90 ± 12.83	53.90 ± 31.59	7.51E-01	87.20 ± 16.80	50.90 ± 12.83	4.00E-05***	55.30 ± 21.10	53.90 ± 31.59	9.09E-01
	NSR	Number of Seminal Roots	4.10 ± 1.45	6.60 ± 1.35	1.00E-03***	7.30 ± 1.16	8.20 ± 1.62	1.23E-01	4.10 ± 1.45	7.30 ± 1.16	4.00E-05***	6.60 ± 1.35	8.20 ± 1.62	2.74E-02*
	LSR	Length of Seminal Roots (cm)	27.70 ± 13.38	43.50 ± 14.01	1.00E-02**	21.33 ± 10.31	53.90 ± 20.85	1.00E-03***	27.70 ± 13.38	21.33 ± 10.31	2.48E-01	43.50 ± 14.01	53.90 ± 20.85	2.07E-01

* P<0.05; ** P<0.01; *** P<0.001.

Table 2. Estimation of phenotypic traits in teosinte *parviglumis* grown in absence and presence of heavy metal stress.

			T. *parviglumis*		
			Cu/Cd (-)	Cu/Cd (+)	
		Description	**Mean ± SD**	**Mean ± SD**	**P value**
Aerial traits	LIL	Length of Immature Leaf (cm)	71.30 ± 11.92	56.25 ± 7.80	5.70E-02
	SB	Stem Branches	5.30 ± 1.83	0.60 ± 0.84	2.00E-04***
	DWAP	Dry Weight of Aerial Part (g)	133.49 ± 28.28	82.72 ± 11.67	7.43E-01
	NFI	Number of Female Inflorescences	1.80 ± 0.63	3.90 ± 166	6.70E-02
	LFI	Length of Female Inflorescences (cm)	15.40 ± 1.35	12.50 ± 2.12	6.50E-02
Roots traits	NBR	Number of Brace Roots	10.60 ± 6.13	11.60 ± 4.55	1.21E-01
	LBR	Length of Brace Roots (cm)	20.00 ± 11.49	2.88 ± 0.66	4.50E-03**
	NCR	Number of Crown Roots	12.80 ± 4.34	9.60 ± 1.43	2.00E-04***
	LCR	Length of Crown Roots (cm)	60.70 ± 16.95	62.80 ± 14.10	2.22E-01
	NNR	Number of Nodal Roots	16.20 ± 4.69	14.00 ± 3.20	3.90E-03**
	LNR	Length of Nodal Roots (cm)	83.00 ± 15.76	104.00 ± 8.46	1.60E-03***

** P<0.01; *** P<0.001.

Appendix

Article title: The influence of heavy metal stress on the evolutionary transition of teosinte to maize

Authors: Jonathan Acosta-Bayona, Miguel Vallebueno-Estrada, and and Jean-Philippe Vielle-Calzada

Figure S1. Cumulative plot of QTL detected in a region of chromosome five that includes *ZmSKUs5* and *ZmHMA1* (modified from Lemmon and Doebley, 2014).

Figure S2. Comparison of chromosome 5 nucleotide variability between maize landraces and teosinte *parviglumis*.

Figure S3. Large scale transcriptional comparison of HM response genes across six maize experiments based on fold change >1 and false discovery rate (FDR) < 0.05.

Figure S4. Expression of *ZmHMA1* in wild-type and homozygous *zmhma1* maize individuals.

Figure S5. Distribution of soils of volcanic origin (andosols; pink) in geographic regions of teosinte *parviglumis* populations most closely related to extant maize.

Figure S6. Speculative model illustrating the influence of heavy metal stress on the evolutionary transition of teosinte *parviglumis* to maize.

Table S1. Additional estimation of phenotypic traits in teosinte *parviglumis* grown in absence or presence of heavy metal stress.

Table S2. Additional estimation of phenotypic traits in wild-type and *zmhma1* maize grown in absence or presence of heavy metal stress.

Table S3. Full comparison of phenotypic values for wild-type W22, *zmhma1*, and teosinte *parviglumis* individuals grown under absence or presence of heavy metal stress

Table S4. Nucleotide variability across the *ZmSKUS5, ZmHMA*1 and *ZmHMA7* locus; and their upstream and downstream neighboring genes in maize landraces, maize improved lines, and teosinte *parviglumi*s accessions included in HapMap3.

Table S5. Description of six transcriptomes reporting HM response genes under different growing conditions and developmental stages.

Table S6. Collection of primers used in this study.

Table S7. Maize landrace accessions used in the genetic diversity analysis chr5.

Table S8. Teosinte *parviglumis* accessions used in the genetic diversity analysis chr5.

Supplementary Files.

Supplementary File 1. List of domestication genes present on chr5 as defined by Hufford et al. 2012

Supplementary File 2. FC and FP values for all domestication genes present in chr5.

Supplementary File 3. FC and FP values of neutral regions included in chr5.

Supplementary File 4. FC and FP values of candidate genes *ZmHMA1*, *ZmHMA7* and *ZmSKUs5.*

Supplementary File 5. FC and FP values of *ZmHMA1*, *ZmHMA7* and *ZmSKUs5* neighboring genes

Supplementary File 6. Genetic diversity across 11.47 Mb of chr.5 in the genomic region comprised between *ZmSKUs5* and *ZmHMA1*.

Supplementary File 7. Genetic diversity in loci encompassing heavy metal response genes shared by six transcriptomes with fold change strictly higher than 1 and FDR<0.05

Figure S1. Cumulative plot of QTL detected in a region of chromosome five that includes *ZmSKUs5* and *ZmHMA1* (modified from Lemmon and Doebley, 2014). Molecular marker positions and gene location of *ZmSKUs5* and *ZmHMA1* are in centimorgans. Abbreviated QTLs are in the left margin. The 1.5-LOD support intervals for QTLs are in black horizontal bars and peak LOD scores in vertical lines. Hatched bars indicate interacting QTLs. Gray vertical shadings indicate the presence of a QTL cluster.

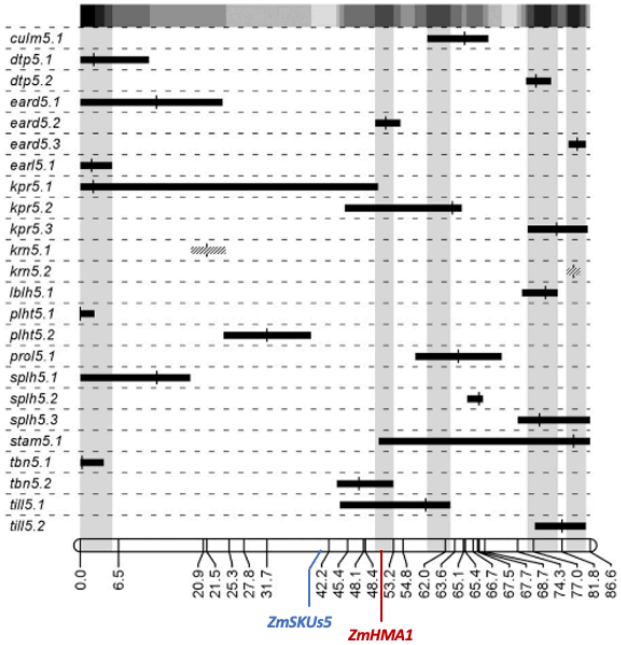

culm: diameter of culm
dtp: days to pollen shed
eard: ear diameter
earl: ear length
kpr: kernels per rank
krn: kernel row number
lblh: primary lateral branch legth
plht: plant height
prol: prolificacy, ears on lateral branch
splh: spikelet length
stam: % of staminate spikelets
tbn: tassel branch number
till: tillering index

Figure S2. Comparison of chromosome 5 nucleotide variability between maize landraces and teosinte *parviglumis*. Violin plots represent all neutral regions comprised chromosome 5 (blue), domestication genes previously reported in chromosome 5 (Hufford et al., 2012; green), the three candidate genes in this study (white), and their six neighboring genes (red). ANOVA-Tukey tests are represented by letters.

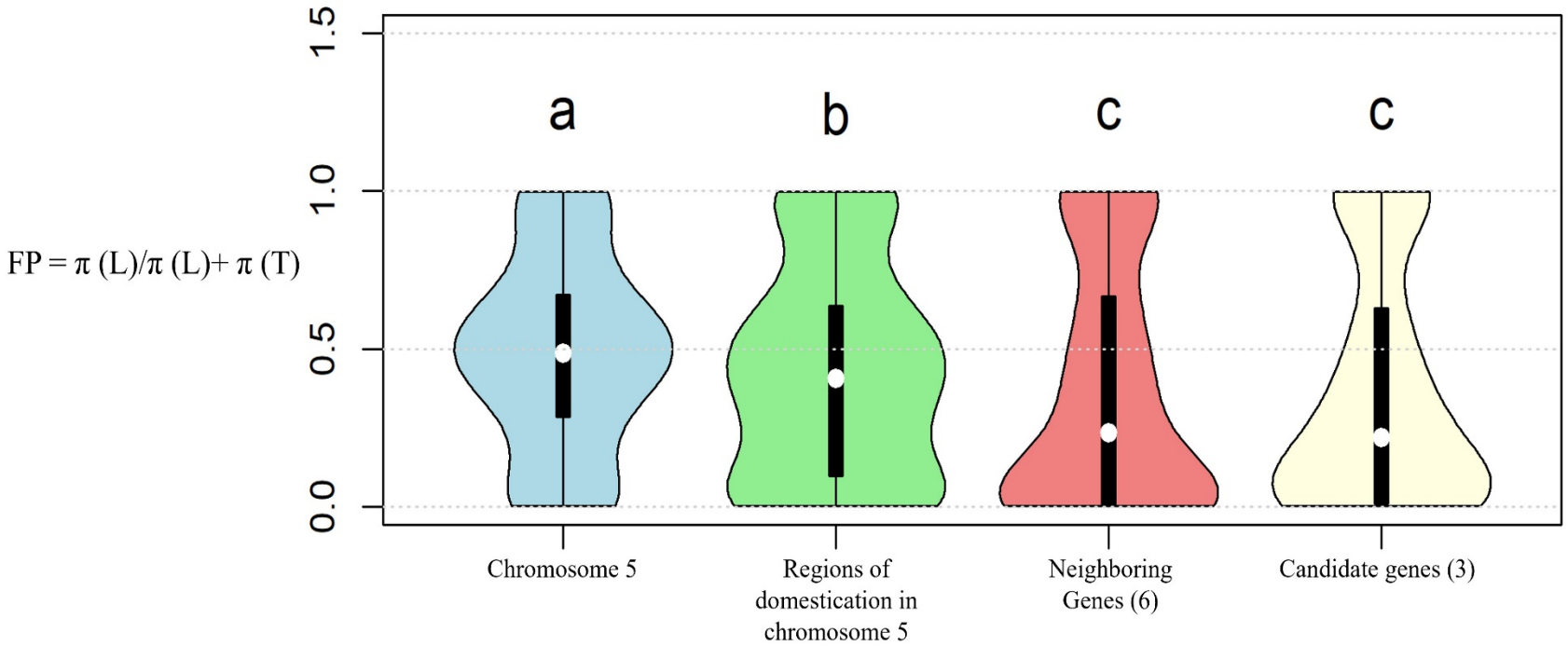

Figure S3. Large scale transcriptional comparison of HM response genes across six maize experiments based on fold change >1 and false discovery rate (FDR) < 0.05. Black dots mark the column of individual transcriptomes, and vertical black lines mark pairwise comparisons between two different transcriptomes included in the histogram. The red vertical red line indicates the column corresponding to common HM response genes included in all six transcriptomes.

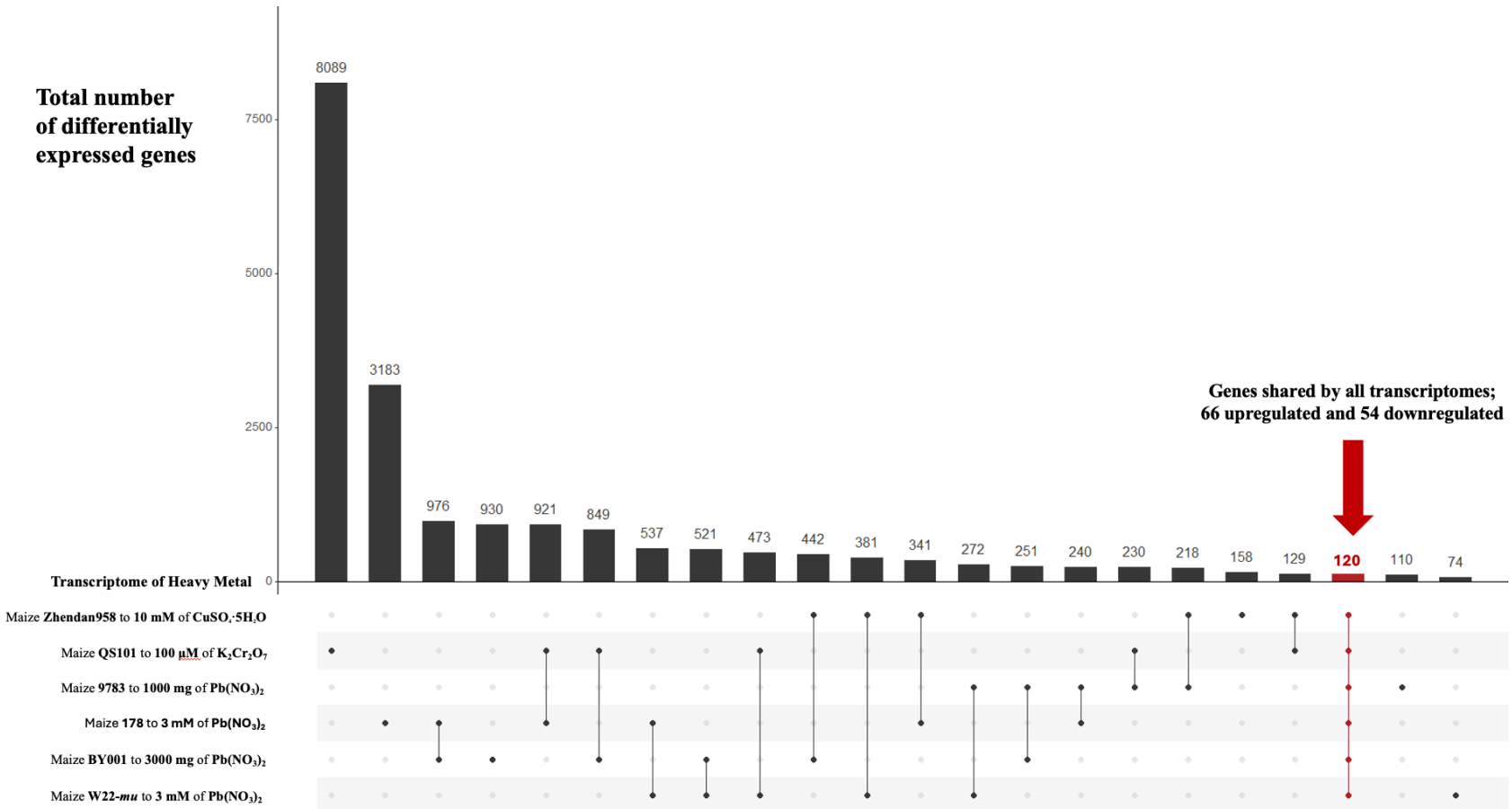

Figure S4. Expression of *ZmHMA1* in wild-type and homozygous *zmhma1* maize individuals. A fragment of *ZmHMA1* was the target of RT-PCR amplification in fourteen W22 wild-type and fourteen *zmhma1* homozygous individuals. *ZmCDK* was used as a positive control in Wild-type individual number 1. A reaction without cDNA addition was used as a negative control. Corresponding primers are presented in Table S7.

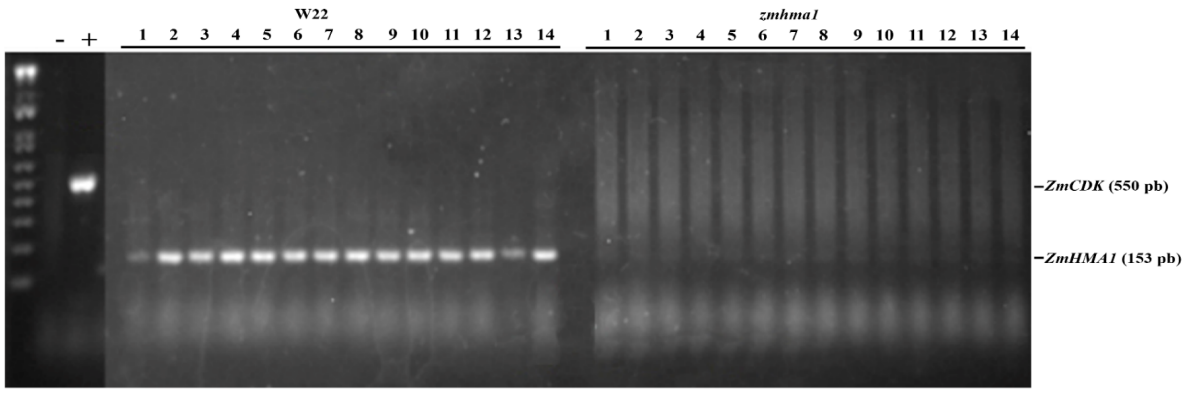

Figure S5. Distribution of soils of volcanic origin (andosols; pink) in geographic regions of teosinte *parviglumis* populations most closely related to extant maize. Andosols are illustrated in pink, teosinte *parviglumis* accesssions represented in Fig. 5a are marked by black asterisks. The Nevado de Toluca and Popocatéptl craters are maked by a red and brown circle, respectively. Adapted from Mapas de INEGI, Edafología (2025). *https://www.inegi.org.mx/temas/edafologia/*

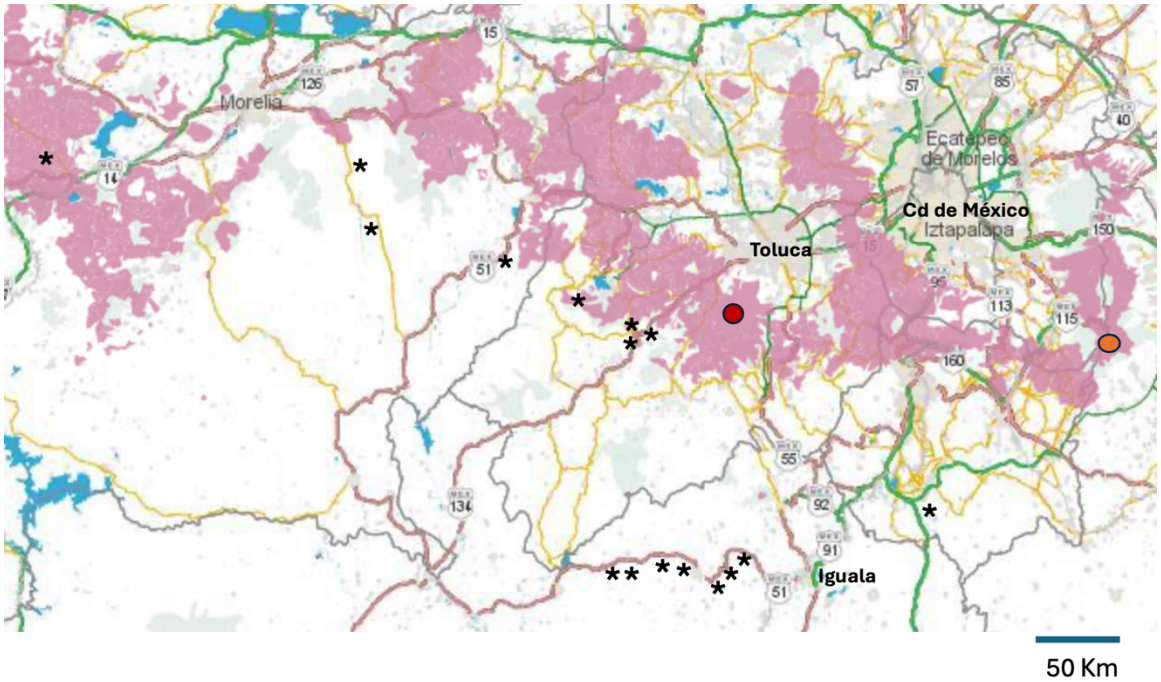

Figure S6. Model illustrating the influence of heavy metal stress on the evolutionary transition of teosinte *parviglumis* to maize.

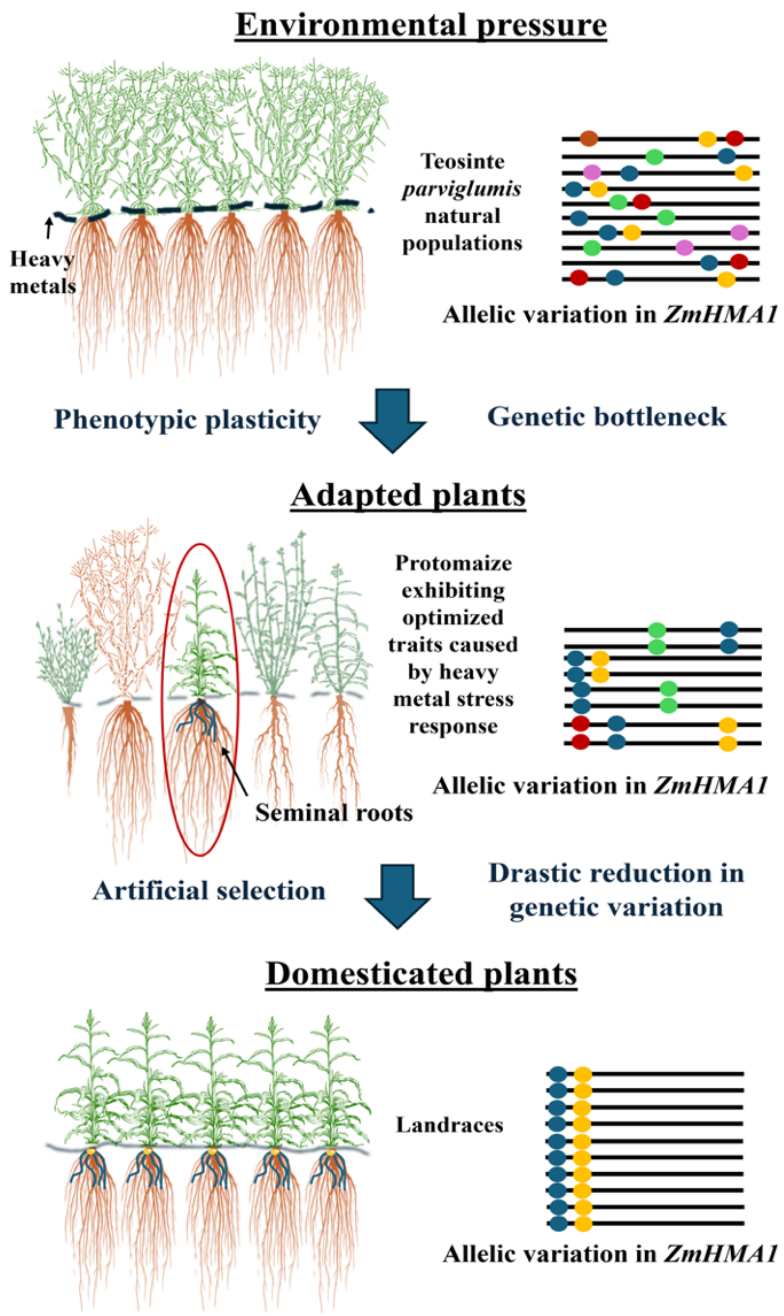

Table S1 Additional estimation of phenotypic traits in teosinte *parviglumis* grown in absence or presence of heavy metal stress.

			Cu/Cd(-)		Cu/Cd(+)		
		Description	**Mean**	**SD**	**Mean**	**SD**	**P Value**
Aerial traits	NL	Number of Leaves	11.00	2.21	11.40	1.71	0.0360*
	LML	Length of Mature Leaf	84.50	4.74	81.30	8.33	0.1662
	WML	Width of Mature Leaf	5.45	0.50	6.00	1.25	0.4685
	WIL	Width of Immature Leaf	7.10	1.02	6.90	0.61	0.0650
	NN	Number of Nodes	9.30	0.95	9.80	1.55	0.0770
	HEI	Height	127.30	27.33	134.56	18.51	0.2648
	SD	Stem Diameter	2.94	0.66	3.12	0.46	0.0130**
	FWAP	Fresh Weight of Aerial Part	667.04	141.02	358.94	49.84	0.7397
	NSB	Number of Spike Branches	22.10	4.75	24.70	4.90	0.1323
	LLBS	Length of Longest Branch in Spike	21.25	4.57	20.80	5.95	0.3917
Root traits	TRL	Total Root Length	105.10	7.10	94.34	44.47	0.3021
	FWR	Fresh Weight of Complete Root System	244.60	101.99	225.70	40.05	0.0892
	DWR	Dry Weight of Complete Root System	34.21	14.29	31.84	3.57	0.0892

* $P<0.05$; ** $P<0.01$.

Table S2 Additional estimation of phenotypic traits in wild-type and *zmhma1* maize grown in absence or presence of heavy metal stress.

			Cu/Cd(-)					Cu/Cd(+)				
			W22		*zmhma1*			W22		*zmhma1*		
		Description	**Mean**	**SD**	**Mean**	**SD**	**P value**	**Mean**	**SD**	**Mean**	**SD**	**P value**
Aerial traits	NN	Number of Nodes	11.00	2.36	10.50	1.35	0.56800	9.10	2.18	10.10	1.52	0.25038
	FWAP	Fresh Weight of Aerial Part	242.56	105.73	218.93	73.36	0.56867	226.39	108.55	318.78	145.03	0.12420
	LLBS	Length of Longest Branch in Spike	21.60	1.66	17.85	4.59	0.02596*	20.45	3.74	15.75	6.99	0.07720
	LFI	Length of Female Inflorescences	24.20	2.97	24.10	3.38	0.94479	21.50	3.17	25.50	4.60	0.03618*
Root traits	TRL	Total Root Length	91.90	17.12	72.29	9.51	0.00535**	83.98	16.19	82.33	17.27	0.82821
	FWR	Fresh Weight of Complete Root System	162.20	76.45	78.76	26.24	0.00431**	104.14	47.28	79.85	31.95	0.19497
	DWR	Dry Weight of Complete Root System	6.81	3.21	5.51	1.84	0.28136	4.37	1.98	5.59	2.24	0.21342

P<0.05; ** P<0.01

Table S3 Full comparison of phenotypic values for wild-type W22, *zmhma1*, and teosinte *parviglumis* individuals grown under absence or presence of heavy metal stress.

			W22				*zmhma1*				Teosinte *parviglumis*			
			Cu/Cd(-)		Cu/Cd(+)		Cu/Cd(-)		Cu/Cd(+)		Cu/Cd(-)		Cu/Cd(+)	
		Description	**Mean**	**SD**	**Mean**	**SD**	**Mean**	**SD**	**Mean**	**SD**	**Mean**	**SD**	**Mean**	**SD**
Aerial traits	NL	Number of Leaves	13.40	0.84	12.00	1.70	11.40	0.84	11.10	0.74	11.00	2.21	11.40	1.71
	LML	Length of Mature Leaf	77.40	6.64	72.35	8.81	69.85	9.18	63.85	7.31	84.50	4.74	81.30	8.33
	WML	Width of Mature Leaf	6.75	1.30	7.20	1.42	9.75	1.40	9.95	0.86	5.45	0.50	6.00	1.25
	LIL	Length of Immature Leaf	59.50	6.10	51.90	9.97	48.25	6.88	45.35	9.43	71.30	11.92	56.25	7.80
	WIL	Width of Immature Leaf	7.45	0.80	6.60	1.10	9.25	0.72	8.85	0.85	7.10	1.02	6.90	0.61
	NN	Number of Nodes	11.00	2.36	9.10	2.18	10.50	1.35	10.10	1.52	9.30	0.95	9.80	1.55
	HEI	Height	99.60	32.61	82.20	34.94	103.15	10.76	125.90	18.81	127.30	27.33	134.56	18.51
	SD	Stem Diameter	3.24	0.52	2.60	0.53	3.02	0.51	2.86	0.59	2.94	0.66	3.12	0.46
	SB	Stem Branches	ND	ND	ND	ND	ND	ND	ND	ND	5.30	1.83	0.60	0.84
	FWAP	Fresh Weight of Aerial Part	242.56	105.73	226.39	108.55	218.93	73.36	318.78	145.03	667.04	141.02	358.94	49.84
	DWAP	Dry Weight of Aerial Part	18.43	8.04	17.22	8.26	28.46	9.54	41.44	18.85	133.49	28.28	82.72	11.67
	NSB	Number of Spike Branches	9.00	1.63	7.20	3.16	13.40	2.32	13.60	1.96	22.10	4.75	24.70	4.90
	LLBS	Length of Longest Branch in Spike	21.60	1.66	20.45	3.74	17.85	4.59	15.75	6.99	21.25	4.57	20.80	5.95
	NFI	Number of Female Inflorescences	1.20	0.42	0.70	0.67	1.90	0.32	1.60	0.52	1.80	0.63	3.90	1.66
	LFI	Length of Female Inflorescences	24.20	2.97	21.50	3.17	24.10	3.38	25.50	4.60	15.40	1.35	12.50	2.12
	WFI	Weight of Female Inflorescences	40.06	14.39	37.75	18.83	69.53	11.20	76.06	25.04	1.29	0.74	1.29	0.56
Root traits	NBR	Number of Brace Roots	12.90	4.33	16.30	4.99	10.60	6.29	9.50	6.79	10.60	6.13	11.60	4.55
	LBR	Length of Brace Roots	16.15	9.75	4.00	2.04	15.75	14.03	2.67	2.01	20.00	11.49	2.88	0.66
	NCR	Number of Crown Roots	11.30	2.11	7.60	0.97	12.10	2.42	9.00	2.58	12.80	4.34	9.60	1.43
	LCR	Length of Crown Roots	58.90	21.87	48.85	11.80	50.50	13.44	44.40	20.75	60.70	16.95	62.80	14.10
	NNR	Number of Nodal Roots	10.50	2.27	6.70	2.79	8.50	2.42	8.00	1.56	16.20	4.69	14.00	3.20
	LNR	Length of Nodal Roots	87.20	16.80	55.30	21.10	50.90	12.83	53.90	31.59	83.00	15.76	104.00	8.46
	NSR	Number of Seminal Roots	4.10	1.45	6.60	1.35	7.30	1.16	8.20	1.62	ND	ND	ND	ND
	LSR	Length of Seminal Roots	27.70	13.38	43.50	14.01	21.33	10.31	53.90	20.85	ND	ND	ND	ND
	TRL	Total Root Length	91.90	17.12	83.98	16.19	72.29	9.51	82.33	17.27	105.10	7.10	94.34	44.47
	FWR	Fresh Weight of Complete Root System	162.20	76.45	104.14	47.28	78.76	26.24	79.85	31.95	244.60	101.99	225.70	40.05
	DWR	Dry Weight of Complete Root System	6.81	3.21	4.37	1.98	5.51	1.84	5.59	2.24	34.21	14.29	31.84	3.57

Table S4 Nucleotide variability across the *ZmSKUS5, ZmHMA*1 and *ZmHMA7* locus; and their upstream and downstream neighboring genes in maize landraces, maize improved lines, and teosinte *parviglumi*s accessions included in HapMap3.

			Upstream(30Kb)			Coding Region			Downstream(30Kb)		
Gene ID	GeneLength(Kp)	DistanceOfGene(Kp)	π(Maize)	π(Teosinte)	**πM/πT**	π(Maize)	π(Teosinte)	**πM/πT**	π(Maize)	π(Teosinte)	**πM/πT**
GRMZM2G375607[a]	0.17	37.3	0.00105	0.000675	1.5556	0.037894	0.0304718	1.2436	0.00041	0.00064	0.6406
GRMZM2G076985[b]	4.17	-	0.011884529	0.017749593	0.669566282	0.000437979	0.007541557	0.058075436	0.002030405	0.006264344	0.324120984
GRMZM2G014508[c]	22.8	97.2	0.00844561	0.005282053	1.598925645	0.037149063	0.011257665	3.299890491	0.002433718	0.017648094	0.13790262
GRMZM2G367857[d]	8.72	25.7	0.005243813	0.006394847	0.820006014	0.008991137	0.011367691	0.790937843	0.002425106	0.006884682	0.352246578
GRMZM2G067853[e]	21.6	-	0.01329488	0.01772011	0.750270738	0.005748	0.0010578	5.433919455	0.00096874	0.0024874	0.389458873
GRMZM2G067883[f]	0.78	24.9	0.005048118	0.007825611	0.645076531	0.00119172	0.000102418	11.63584526	0.003030221	0.00681471	0.444658834
GRMZM2G374375[g]	1.84	228.6	0.0007481	0.000974	0.768069815	0.00974	0.01495	0.651505017	0.00054	0.00948	0.056962025
GRMZM2G029951[h]	4.5	-	0.000678	0.010784	0.06287092	0.00015	0.00148	0.101351351	0.00066	0.00454	0.145374449
GRMZM2G701784[i]	0.54	56	0.0005974	0.009748	0.061284366	0.00074	0.01784	0.041479821	0.00017	0.00009	1.888888889
GRMZM2G067919[j]	2.4	-	0.00611	0.00809	0.755253399	0.01035	0.01058	0.97826087	0.01417	0.01254	1.129984051

[a]Uncharacterized gene; [b]*ZmSKUS5* (Multicopper oxidase); [c]*ZmDds_sub1* (Decaprenyl-diphosphate synthase subunit 1); [d]Uncharacterized gene; [e]*ZmHMA1;* [f]Uncharacterized gene; [g]*Zmpgl20* (Exopolygalacturonase-like); [h]*ZmHMA7*; [i]Uncharacterized gene; [j]*ZmGLB1* (Globulin1)

Table S5. Description of six transcriptomes reporting heavy metal response genes under different growing conditions and developmental stages.

	Experimental design	Analysis	DEGs[a] upregulated	DEGs[a] downregulated	Statistics	Reference
1	Mutant lines of ZmbZIP54-OE and zmbzip54 were compared with W22 as control. Plants in V2 were transferred to the modified Hoagland solution supplemented with 3 mM Pb(NO3)2 for 48 h	Root Transcriptome	437	180	Gene expression was calculated using FPKM. Genes that exhibited fold change ≥1 and false discovery rate (FDR) < 0.05 were considered differentially expressed.	Fengxia, H et al., 2025. Complex regulatory network of ZmbZIP54-mediated Pb tolerance in maize. *Plant Physiology and Biochemistry* 224:109945
2	Seven-day-old seedlings of the maize hybrid line Zhendan958 were grown in Petri dishes supplemented with 0.5- or 10-mM Cu for 1 week, seedlings without Cu were used as control	Root Transcriptome	362	257	Gene expression was calculated using FPKM and differential expression was estimated using DESeq2. Genes that exhibited fold change >2 and an adjusted p-value 0.05 were considered differentially expressed.	Zhang, M et al., 2024. Comparative transcriptome analysis of maize (*Zea mays* L.) seedlings in response to copper stress. *Open Life Sciences* 19(1): 20220953.
3	Maize inbred line BY001, in V2 stage were treated with modified Hoagland solution containing different Pb concentrations. The Pb(NO3)2 concentrations were 0 (control), 500, 1000, 2000 and 3000 mg/l for 48 h	Root Transcriptome	1356	577	Gene expression was calculated using FPKM and differential expression was estimated using DESeq2. Genes that exhibited fold change ≥1 and false discovery rate (FDR) < 0.05 were considered differentially expressed.	Zhang, X et al., 2024. Transcriptomics combined with physiology and metabolomics reveals the mechanism of tolerance to lead toxicity in maize seedlings. *Physiologia Plantarum* 176: e14547.
4	Maize plants of QS101 a Cr-sensitive cultivar of three weeks were transplanted to nutrient solution with 100 µM of K2Cr2O7 to induce Cr stress for seven days, plants without treatment were used as control	Root Transcriptome	3988	5156	Gene expression was calculated using FPKM and differential expression was estimated using Cuffinks software. Genes that exhibited fold change >1 and false discovery rate (FDR) < 0.05 were considered differentially expressed.	Yang, X et al., 2023. Melatonin alleviates chromium toxicity in maize by modulation of cell wall polysaccharides biosynthesis, glutathione metabolism, and antioxidant capacity. *Int. J. Mol. Sci.* 24(4): 3816.

5	Seedlings of maize inbred line 9782, were randomly divided into two groups, CK–grown seedlings, grown only in half-strength Hoagland solution, Pb1000–grown in CK + Pb1000 (1000 mg L−1 Pb(NO3)2) for Pb stress for 12, 24 and 48 h	Root Transcriptome	195	189	Gene expression was calculated using FPKM and differential expression was performed using Cuffinks software. Genes that exhibited fold change >1 and false discovery rate (FDR) < 0.001 were considered differentially expressed.	Gao, J et al., 2015. The development dynamics of the maize root transcriptome responsive to heavy metal Pb pollution. *Bio.Biophysical Research Comm. 458(2): 287-293.*
6	Seedlings of maize inbred line 178, were randomly divided into two groups, one was transferred to a fresh control solution, and the other was transplanted into an identical solution but containing 3 mM Pb(NO3)2 for 24, 48 and 72 h	Root Transcriptome	2379	1832	A combination of FDR < 0.001 and the absolute value of log2 Ratio ≥ 1 were used as the threshold to determine the significance of gene expression difference, between compared libraries.	Shen, Y et al., 2012. Genome expression profile analysis reveals important transcripts in maize roots responding to the stress of heavy metal Pb. *Physiologia Plantarum* 147(3): 270-282.

[a] Differentially expressed genes

Table S6. Collection of primers used in this study.

Primer Name	Gene ID	Forward	Reverse
*ZmHMA1*_PCR/qPCR	GRMZM2G067853_T02	TGAACACTCCGACATGGTCC	GGTGTAGCTTGAGGGAGAGC
*ZmHMA7*_PCR/qPCR	GRMZM2G029951_T01	ATCTCCTGCGCTTCTTGTGC	CCTCTGGCCTGTACTGAACC
*ZmTb1*_qPCR	Zm00001eb054440	CCCATGGACTTACCGCTTTA	GGGAGCATGGGTAGCAGTAG
*ZmCDK*_PCR	Zm00001eb215750_T001	GGAAGGTATGCACAGGACAGAT	TTCAGCACAATCTTGGCAAAAC
*ZmCDK*_qPCR	Zm00001eb215750_T001	CCGTCATCGCCTCACGAAGAG	AGAGCCTGCCTTACGGAATTGG
ZmHMA1 genotyping	GRMZM2G067853_T02	GACGACACAAGCCAAAACAG	AGGGAGATGCAGCAGAGGT

Table S7. Maize landrace accessions used in the genetic diversity analysis of chr5.

1	BKN009
2	BKN010
3	BKN011
4	BKN014
5	BKN015
6	BKN016
7	BKN017
8	BKN018
9	BKN019
10	BKN020
11	BKN022
12	BKN023
13	BKN025
14	BKN026
15	BKN027
16	BKN029
17	BKN030
18	BKN031
19	BKN032
20	BKN033
21	BKN034
22	BKN035
23	BKN040

Table S8. Teosinte *parviglumis* accessions used in the genetic diversity analysis of chr5.

1	TIL01
2	TIL01-JD
3	TIL02
4	TIL03
5	TIL04-TIP285
6	TIL04-TIP454
7	TIL05
8	TIL06-TIP260
9	TIL06-TIP496
10	TIL07
11	TIL09
12	TIL10
13	TIL11
14	TIL12
15	TIL14-TIP498
16	TIL15
17	TIL16
18	TIL17